UNIVERSITÀ
DEGLI STUDI
DI PADOVA

Head Office: Università degli Studi di Padova

Department of Civil, Environmental and Architectural Engineering (ICEA Dept.)

Ph.D. COURSE IN:
SCIENZE DELL'INGEGNERIA CIVILE ED AMBIENTALE
XXXI CICLO

Numerical Optimization of the Neochord Mitral Valve Repair Procedure

Thesis written with the financial contribution of Fondazione Cariparo and Fondazione Ing. A. Gini

Coordinator: Prof. Marco Marani

Supervisor: Prof.ssa Francesca Maria Susin
Co-Supervisor: Prof. Paolo Peruzzo

Ph.D. student: Luigi Di Micco

Accademic year: 2017/2018

Table of Contents

Acknowledgments (ITA)

Un ringraziamento speciale va a coloro che hanno reso possibile questo lavoro di tesi: in particolare a **Francesca**, che ha creduto in me e mi ha dato la possibilità di poter affrontare quest'esperienza di dottorato; mi hai insegnato che quello che facciamo è importante e va fatto con impegno e passione ma che nella vita ci sono cose molto più importanti alle quali prestare sempre attenzione; **Paolo**, presente in ogni momento e che ha contribuito in maniera fondamentale alla riuscita della tesi; **Andrea Colli**, super cardiochirurgo e uomo dal carattere incredibile, grazie per gli insegnamenti ed il fondamentale supporto clinico, tutto quello che so dal punto di vista clinico lo devo a te; **Daniela Boso**, per l'enorme aiuto nella fase più delicata di tutto il lavoro, sei stata molto preziosa per me; **Benedetta Biffi**, tutta la seconda parte della tesi è merito tuo; un grazie enorme a te e a **Silvia Schievano** per il bel lavoro fatto; **Gaetano Burriesci** è stato un piacere far parte del tuo laboratorio per 6 mesi, grazie per i consigli e per il lavoro fatto insieme.

Grazie anche ai due revisori del lavoro di tesi, **Gianni Pedrizzetti** e **Andrea Avanzini**. Grazie per il tempo che avete dedicato alla revisione e per i fondamentali consigli per migliorare ulteriormente il lavoro.

Grazie a tutti quelli che hanno reso l'esperienza di Londra fantastica sia dal punto di vista lavorativo che umano, è stato un'enorme piacere condividere del tempo con voi, non vi dimenticherò molto facilmente: **Gaetano B., Andrea D., Ben, Anna Maria, Giorgia, Andrea, Antonio, Selim, Master Giacomo & Master Wenbo**.

Grazie a tutti i compagni d'ufficio Padovani che in questi anni si sono rivelati amici oltre che colleghi: **Ponzio, Ingenui (Alessandro & Tommaso), Sergio, Marta, Arianna, Giulia**. Ho condiviso delle belle esperienza con voi e spero ci saranno molte altre occasioni per stare assieme.

Grazie anche a tutto il XXXI ciclo di dottorato con il quale ho iniziato quest'esperienza, auguro a tutti voi di fare grandi cose: **Chiara C., Chiara F., Claudio, Marta, Silvia e Victor**.

ABSTRACT

The heart has four heart valves (HV), and correct HV function is the main prerogative for the vital of cardiovascular health. The mitral valve (MV), the largest valve of the heart, regulates unidirectional flow between the left atrium and left ventricle. During the systolic phase the MV function is to sustain the maximum ventricle pressure and prevent the reversal flow; during the diastole, the MV is open allowing the blood flow from the atrium and the ventricle filling. The physiological function of the left heart is partly guaranteed by the perfect sealing of the mitral valve in the systole. In presence of disease due to the prolapse of the valve leaflets, instead, there is a persistent regurgitation from the ventricle to the atrium.

The degenerative mitral valve regurgitation (DMR) is one of the most common valvular heart diseases that affects about 4% of the population over 70; the natural history of severe MR is adverse, leading to worsening of left ventricle (LV) function, pulmonary hypertension, atrial fibrillation, and death.

A variety of less invasive treatment for degenerative MV has been developed. Among these, the NeoChord procedure has emerged as the most promising intervention to repair MV. In NeoChord technique, artificial chords are placed through percutaneous access to restore the proper closure of the leaflets and consequently mitigate the regurge.

The present work focuses on the numerical investigation of the Neochord procedure by means of a finite element model, which firstly analyses an idealized anatomy of prolapsing MV and, subsequently, investigates the procedure on three patient-specific MV anatomies. For the first time, the intraoperative phase of the procedure was studied considering two modes of chords tensioning. In additions, we studied on the patients-specific domains the role of both the access site correlated to the suture trajectories inside the left ventricle and the different stitching points on the prolapsed leaflet, by performing a consistent number of simulations. Numerical simulations are commonly used to assess the effectiveness and capability of surgical procedures. For this reason, the proposed study get an insight also on the commonly reported procedural complications, such as *i)* the leaflet rupture, *ii)* the interference of the artificial suture with the MV structures, and *iii)* the neochords overloading/unloading. The present model lays the basis for the realization of a numerical tool dedicated for the surgical planning, which would like to support the surgeons to point out the potential critical issues due to the patient-specific features of the MV undergoing treatment, making it possible the optimum design of the procedure.

SOMMARIO

Il cuore è composto da quattro valvole cardiache. La loro corretta funzione è necessaria per garantire costantemente un adeguato apporto di sangue all'intero sistema cardiocircolatorio. Tra le quattro valvole la più grande è la valvola mitrale, che è posta a presidio tra l'atrio e il ventricolo sinistro. Durante la fase sistolica la valvola mitrale si chiude impedendo il flusso tra le due camere e sostenendo la pressione massima che si sviluppa nel ventricolo sinistro; durante la diastole, invece, la valvola mitrale si apre permettendo il flusso del sangue dall'atrio verso il ventricolo. La fisiologica funzionalità del cuore sinistro è in parte garantita soprattutto dalla perfetta tenuta della valvola mitrale in fase sistolica. Quando ciò non avviene, spesso a causa del prolasso dei lembi della valvola stessa, si assiste al persistere di un flusso di rigurgito dal ventricolo verso l'atrio.

Il rigurgito della valvola mitrale, di tipo degenerativo, è una tra le più comuni patologie cardiache e colpisce circa il 4% della popolazione oltre i 70 anni d'età. L'indesiderato sviluppo di questa patologia, con conseguente peggioramento della funzionalità del ventricolo sinistro, porta ad una serie di complicanze, quali l'ipertensione polmonare e la fibrillazione atriale, e nelle condizioni più gravi alla morte.

Negli ultimi anni sono state maturate una varietà di terapie chirurgiche per trattare efficacemente questa patologia, soprattutto grazie allo sviluppo di nuove metodologie di tipo mini-invasivo. Una delle tecniche più recenti e promettenti è l'impianto di corde artificiali all'interno del ventricolo a supporto dell'esistente struttura valvolare, il cosiddetto impianto di neocorde. In questo tipo di intervento le corde artificiali sono posizionate attraverso un accesso transapicale allo scopo di ripristinale la struttura valvolare originaria e, conseguentemente, la chiusura corretta della valvola.

Il seguente lavoro di tesi si concentra sull'indagine numerica della procedura di riparo Neochord. A questo scopo, è stato sviluppato un modello agli elementi finiti per indagare l'interazione tra le corde artificiali e la valvola mitrale, inizialmente su un modello idealizzato di valvola prolassata e, successivamente, su dei modelli "paziente specifico" ricavati dall'analisi di immagini cliniche (Echo e CT-scan).

È stata studiata per la prima volta il ripristino della valvola mitrale nella fase intraoperatoria della procedura e sono state analizzate due modalità di tensionamento delle suture impiantate. Inoltre, per tre diverse tipologie di prolasso sono stati indagati vari scenari di possibili impianti che tenessero conto dei possibili punti di inserimento delle corde e della traiettoria finale delle stesse.

Parallelamente si è cercato di indagare alcune delle complicanze procedurali comunemente riportate dai cardiochirurghi. Nello specifico, *i)* la rottura dei lembi nel punto di attacco delle corde, dovuta principalmente agli eccessivi stress sul lembo dovuti all'attacco delle suture e al successivo tiro, *ii)* l'eventuale interferenza della sutura artificiale con le strutture della valvola, in particolare con le corde native e i lembi, e *iii)* il sovraccarico/scarico delle suture impiantate.

Il presente modello rappresenta il primo passo verso la realizzazione di uno strumento numerico per la pianificazione chirurgica, che permetta di mettere in evidenza, in fase pre-operatoria, le potenziali criticità legate alle caratteristiche individuali del prolasso trattato, rendendo possibile la messa a punto di una procedura *ad hoc* ottimale.

1 Overview of Heart Physiology

1.1 Introduction

The present thesis project focused, by a series of numerical analysis, on the treatment of the mitral valve prolapse through a less invasive surgical technique, named NeoChord procedure. An exhaustive description of this technique is presented in the next Chapter, but firstly, in this chapter, we present a short description of the human heart and, with a little more detail, we also describe the anatomy, the function and the related diseases of the mitral valve.

The following introduction does not want to go into detail on the clinical aspects of the topic, but rather to give the basic medical knowledge needed to correctly frame the issue of the present dissertation to a Reader having an engineering background. Indeed, the simplifications, the geometrical and mechanical representation adopted, as well as the interpretation of the results of the numerical models strongly depend on the correct comprehension of both the clinical data and the physiology of anatomical district. This chapter summarizes the preliminary knowledge necessary for the development of the mitral valve engineering schematization.

In the first part, after a short description of the human heart and of the cardiac valves, we are interested in the function of the mitral valve in the healthy state and subsequently the characteristics in the dysfunction state. The attention is then focused on the mitral valve prolapse, the main mitral valve dysfunction mechanism on which the entire thesis is concerned.

1.2 The Human Heart

As well known, the human heart is structured in four chamber whose main function is to pump blood throughout the body. Figure 1-1 illustrates schematically the configuration of the heart during all the phases of the cardiac cycle, and the position of the cardiac valves; in addition, the black arrows show the blood direction during a healthy cardiac cycle, while the green arrows indicate the direction of the ventricle contraction.

The heart is the pump of all the cardiovascular system, and consist of a double pump (right side and left side) that works in series to ensure the circulation of the blood, non-oxygenated and oxygenated, in the pulmonary and systemic circulation, respectively. The correct flow direction into the chambers is ensured by the presence of four valves, i.e. the mitral valve, the aortic valve, the tricuspid valve, and the pulmonary valve (see Figure 1-2).

The mitral valve and the tricuspid valve are defined atrioventricular valves, which separate the left and right atria from the left and right ventricles, respectively. The aortic valve and the pulmonary valve are defined semilunar valves and separate the left and right ventricle from the aorta and pulmonary artery, respectively.

During the cardiac cycle, all these valves regulate the unidirectional flow of blood through the heart, enabling the generation of the proper pressure able to pump blood around the cardiovascular system. During the closure phase of the valves, the main functions are to sustain the pressure loads and do not allow reversal flow, whereas during the open phase the valves have to do not obstacle the fluid motion with a rapid transition from close to open.

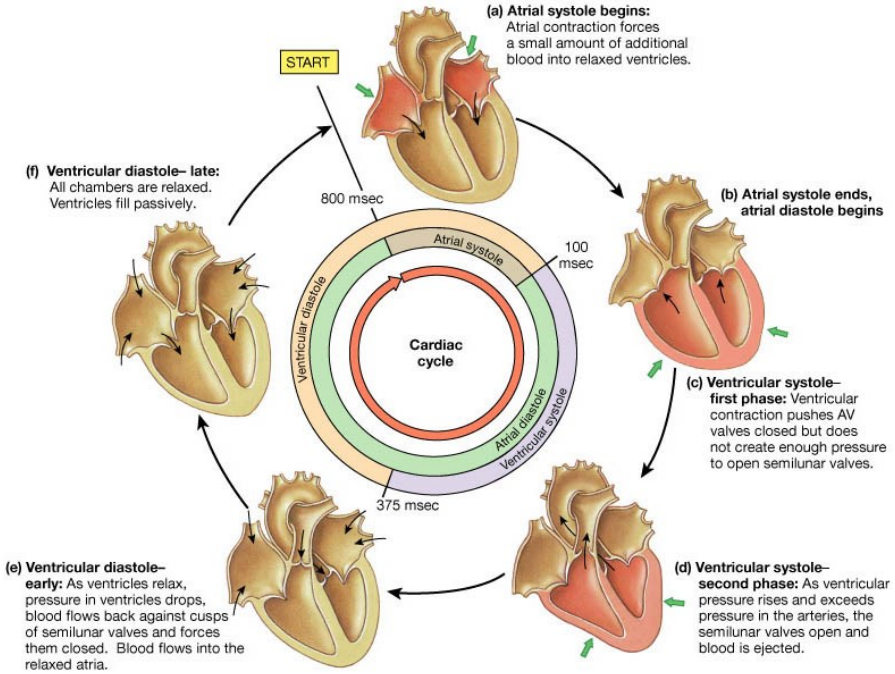

Figure 1-1 *Scheme of the Cardiac Cycle showing all the main atria and ventricles behavior and functions. (http://sites.psu.edu/bio101and141/human-physiology/cardiovascular/)*

Specifically, the right side of the heart supplies the pulmonary circulation, whereas the left side of the heart controls the blood flow in the systemic circulation. The right atrium receives venous blood from superior and inferior vena cavae and during the diastolic phase (ventricular relaxation), the blood flows into the right ventricle through the tricuspid valve. During the systolic phase (ventricular contraction), blood reaches the lung, for the oxygenation, through the pulmonary arteries thanks to the opening of the pulmonary valve. The oxygenated blood returns to the heart via the pulmonary veins into the left atrium. The blood fills the left ventricle thanks to the opening of the mitral valve, during the relaxation

of the ventricle. The subsequent ventricular contraction pumps blood into the systemic circulation via the aortic valve. Figure 1-1 describes all the phases involved in a physiologic cardiac cycle. The label a) indicatively defines the beginning of the cardiac cycle during which occurs the atrial systole. The atrial systole is followed by the atrial diastole (label b) and by the ventricular systole during which we distinguish two small phases (label c and d). The former is called the isovolumetric contraction phase, since the ventricular pressure rises although the closure of the valve persists, i.e. in this phase the ventricle is contracting but its volume does not change. Differently, in phase d), the blood is ejected through the semilunar valves while the pressure, after a first stage of growing, decreases. Phases e) and f) describe the ventricular diastole during which the heart chambers are relaxed and blood can flow into atria and ventricles.

If any changing on the correct functionality of a valve occurs, the heart function previously depicted can be affected by negative feedbacks on the ventricular filling and ejection, with dramatic consequences on the blood supply for the entire cardiovascular system. Often, dysfunctional valves show abnormal leaflets dynamics, in particular during the closure, which are commonly associated with an abnormal retrograde flow and/or abnormal narrowing of the valvular orifice in the open configuration, the so-called valve stenosis.

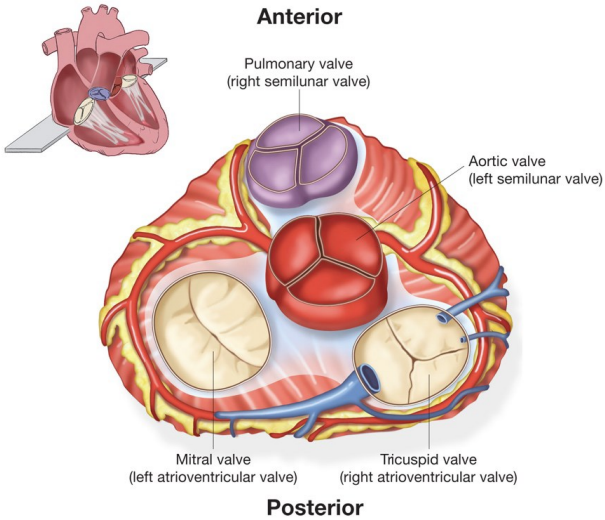

Figure 1-2 *Heart Valves: Cross-section of the heart showing the four valves in a closed position. (https://www.heart-valve-surgery.com/anatomy-valve-problems)*

1.3 The Mitral Valve: Anatomy and Function in Normal State

Among the valves described above, the mitral valve (MV) is the most interesting for this thesis work. The mitral valve structure (see Figure 1-3) consists of an annulus, two leaflets,

a series of branching chordae tendineae and two papillary muscles. All these components have to operate in synergy to guarantee the correct valve functionality, i.e. the mitral valve with the aortic valve has to be able to regulate the flow of the oxygenated blood into the left ventricle and its ejection into the aorta.

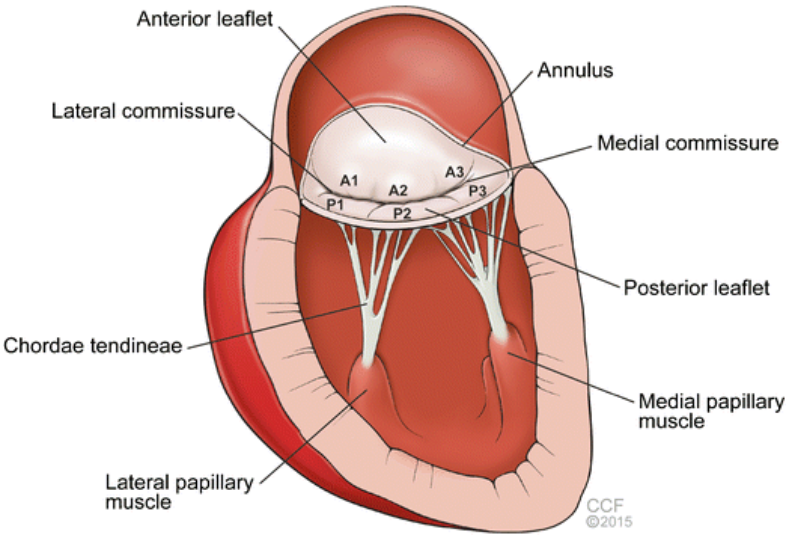

Figure 1-3 *Mitral Valve Anatomy, [1].*

The annulus connects the mitral valve leaflets to part of the structure of the heart; it consists of a fibrous structure that defines the orifice of the valve. Being the mitral valve adjacent to the aortic valve, the annulus shares this fibrous structure with the aortic annulus creating a continuity fibrous structure between these valves. In the normal state, the annulus presents a flexible structure that changes size and shape during the cardiac cycle. In particular, during the diastolic phase, the annulus achieves its maximum area in order to maximize the blood flow into the ventricle, whereas, during the systolic phase the annulus contraction occurs. The annulus shape is almost flat and circular during the ventricular filling, whereas the annulus assumes a "saddle" shape configuration during heart contraction, [2].

The leaflets of the mitral valve are described as a continuous structure of the tissue. They are connected to the annulus structure. According to Figure 1-3, it is possible to subdivide the leaflets tissue into different segments: the anterior, posterior and commissural segments. The anterior segment has a semicircular profile and it usually consists of a single scallop. The anterior leaflets extend along the annulus typically for a third of the annulus perimeter.

The posterior segment is placed in the opposite side, separated by the commissural segments, and it typically presents three scallops, namely P1, P2, and P3.

The area of all the leaflets segments, during the closure phase of the valve, guarantees the seal of the mitral valve orifice, thanks to the contact among leaflets scallop on the atrial surface. Since the leaflets are passive structures, the valve dynamic depends on the difference of pressure between the atrium and ventricle i.e. the pressure drop upstream and downstream the valve.

The chordae tendineae are thin chords structures that support the valve during the closure. In particular, they maintain the leaflets in position during the ventricular contraction and in particular at maximum pressure difference between the two chambers, avoiding that the leaflets can turn inside the atrium out. These chords structures can be classified by its size and insert position on the leaflets body, as following: marginal, rough zone, strut, and basal chordae. The marginal chordae are the thinnest chords and they are attached to the leaflet at the free margin zone. The rough chordae, structurally similar to the marginal chordae, are attached below the free margin and together with the marginal chordae promote the contact between the leaflets during the closure. The strut and basal chordae present different structure and function. Thicker than marginal chords, these structures support the leaflet body from the pressure load developed during the ventricular contraction, [3], [4].

The chordae tendineae can carry out their function thanks to the connection with the ventricular wall via the papillary muscles (see Figure 1-3). The latter are defined as a set of muscle fascicles protruding into the ventricle and they are classified according to their anatomical position as lateral and medial papillary muscles. During the cardiac cycle, the papillary muscles contract and relax to ensure the correct valve closure. In particular, during the systole the papillary muscles contract in order to augment the tension in the chordae tendineae, [5].

1.4 The Mitral Valve: Anatomy and Function in Dysfunction State

As mentioned above, during the cardiac cycle the mitral valve has two main functions, [6], [7], [8]: Sealing of the mitral orifice for preventing the formation of the retrograde flow during the systolic phase (ventricular contraction associated with ventricular high-pressure condition); Facilitating the ventricular filling, during the diastolic phase, by minimizing the flow resistance.

This physiological condition depends on a concomitance of several factors, indeed, changes due to dysfunctions of the biomechanics properties of the valvular tissue as well as

of the pressure load or changing in the functional anatomy, can rapidly resulting in abnormal ventricular filling and ejection.

Mitral valve dysfunction can be classified according to the type of abnormalities observed during the cardiac function. The loss of contact between leaflets during the ventricular contraction that generates a retrograde flow toward the atrium is called *mitral regurgitation.* In this case, the structures of the valve lose efficiency in the sealing of the orifice, accordingly, an un-physiological flow rises into the left atrium (see Figure 1-4). The amount of regurge volume and the jet magnitude and width identify the severity of the dysfunction. The following three classes define the grading of mitral regurgitation: *Mild, Moderate* and *Severe*. A mild regurge is characterized by the presence of a small central jet < 4 cm^2 and a regurgitant volume < 30 ml/bat. The severe mitral regurgitation presents a large central MR jet (area > 40 % of left atrium area) and a regurgitant volume > 60 ml/bat. There are not criteria to correctly define the moderate condition, however in the clinical practice, it ranges between the limits prescribed for the mild and severe conditions, i.e. the regurgitant volume is between 30 and 59 ml/bat [9].

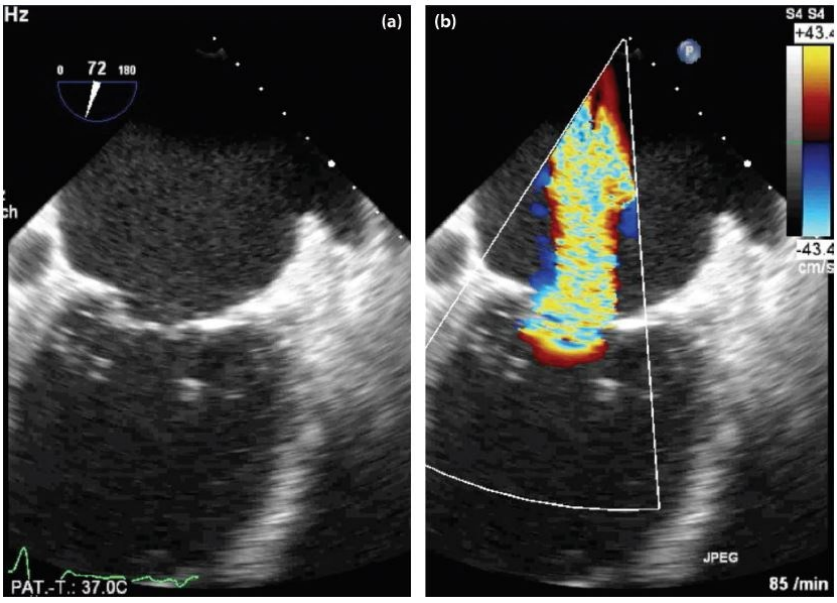

Figure 1-4 *Example of a Mitral regurgitation leading to a retrograde central flow pattern, [10].*

An increased resistance to the blood flow toward the left ventricle during the filling is called *mitral stenosis.* In this circumstance, the tissues of valve stiffen, causing an uncompleted opening of the valve and, hence, an increase of the flow resistance. A clinical assessment of the severity of the stenosis can be evaluated by measuring this reduced area

and consequently by estimating the increased pressure drop upstream through the mitral orifice.

Recommendations for classification of mitral stenosis severity define, [11]: mild severity associated to a valve area > 1.5 cm^2, and mean pressure drop < 5 mmHg; moderate stenosis with mitral valve area between 1-1.5 cm^2, and mean pressure drop between 5-10 mmHg; severe mitral valve stenosis with area < 1 cm^2 and a mean pressure drop > 10 mmHg.

Mitral valve dysfunction usually pertains to all the substructures of the valve. For instance, the annulus, in a prolapsed valve, has reduced mobility during the different phases of the cardiac cycle and, moreover, the reduction of the annulus area from the diastole to systole appears less evident, [2]. This defect of the annulus reduces the capability of the leaflets to keep in contact during the closure and this reduced coaptation can origin the mitral regurge flow into the left atrium.

Alterations in the leaflets tissue lead to an incorrect function of the valve. In particular, changes in the mechanical strength of the leaflets can result not only in an abnormal deformation at the closure proper of the prolapse formation but in some cases also to the thinning of the leaflets, [12].

Similarly to the leaflets structure, loss of mechanical strength of the chordae tendineae leads to an incomplete closure of the leaflets with the generation of prolapse/regurgitation. Same consequence occurs in case of chordae rupture with the formation of the so-called flail, [13].

Finally, also the papillary muscle plays an important role for the correct state of the mitral valve. Indeed The loss of contractility given by this muscle due to its rupture causes a severe regurgitation of the valve, [5]

In summary, every single substructure plays the main role for the correct functionality of the valve. If only one of those presents abnormal behavior the overall apparatus is affected by negative consequences, leading to the vale dysfunction.

1.5 Mitral Valve Insufficiencies: Focus About Mitral Regurgitation (MR)

Mitral regurgitation (MR) is one of the most complex valvular diseases. MR is classified into two categories: the functional and degenerative Mitral regurgitation, [10].

Functional MR (FMR), due to the left ventricular (LV) dilation and dysfunction, occurs in a normal structural mitral valve apparatus, and it is collateral to a degenerative myocardial dysfunction that leads to mitral regurgitation. Typically, in this case, the annulus is dilated and the papillary muscles are spread apart;

Degenerative MR (DMR), due to a structural abnormality of the valve apparatus that prevents proper valve closure, is mainly led, among possible valve failures, to the prolapse or flail, [12], [14], [15]. A degenerative mitral disease is often due to myxomatous degeneration that is associated with abnormalities in collagen and fibrillin. The most evident clinical observation in patients with degenerative valve disease is the leaflet prolapse for the elongation or the rupture of the native chords.

According to Adams et al. [16], mitral valve prolapse due to degenerative failure is described by several MV characteristics, which vary from the simple chords rupture involving prolapse of an isolated segment (typically, valves of small size with only central posterior leaflet affected), to the multi-segment prolapse involving one or both leaflets in valves with a significant excess of tissue and large annulus size. The grade of degenerative disease is shown in Figure 1-5. The spectrum of degenerative disease ranging from fibroelastic deficiency (FED) to Barlow's disease, passing through Forme Fruste. The Fibroelastic deficiency is a condition described by a fibrillin deficiency, which leads to a rupture/elongation of one, or more thinned chordae, mainly. Sometimes, the prolapsing segment develops myxomatous changes causing a proliferative condition of the affected leaflet segment. In the FED condition, adjacent leaflet segments are usually normal and thinned with a valve of normal size.

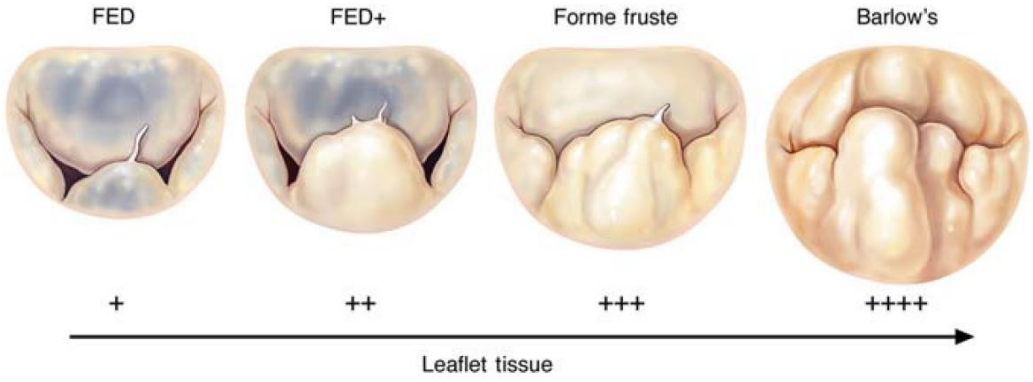

Figure 1-5 *Grade of degenerative mitral disease, [16].*

Dissimilar to FED, Barlow's disease is described by an excess of tissue and valve size generally quite large. In this pathology, in the most of case multi-segments are involved by myxomatous changes. Both diffuse chords rupture end/or elongation and severe annular dilatation with varying degrees of annular calcification are often observed.

1.6 Echocardiographic assessment

From the clinical point of view, the evaluation of a MV pathology, and in particular the definition of the involved leaflets and segments, is commonly determined by the transthoracic echocardiography. A more precise assessment can be instead performed by the transoesophageal echocardiography, once the investigation by means of the transthoracic echocardiography is unsatisfactory to characterized the disease. The use of 3D echocardiography provides additional information to determine the exact localization of lesions. As an example, is reported a new geometrical classification proposed by Colli and co-worker, that come from a precise clinical images analysis and identify with good accuracy a precise assessment of the exact location of the disease, useful for the correct evaluation of the pathology itself (see Figure 1-6,[16], [17], [18]).

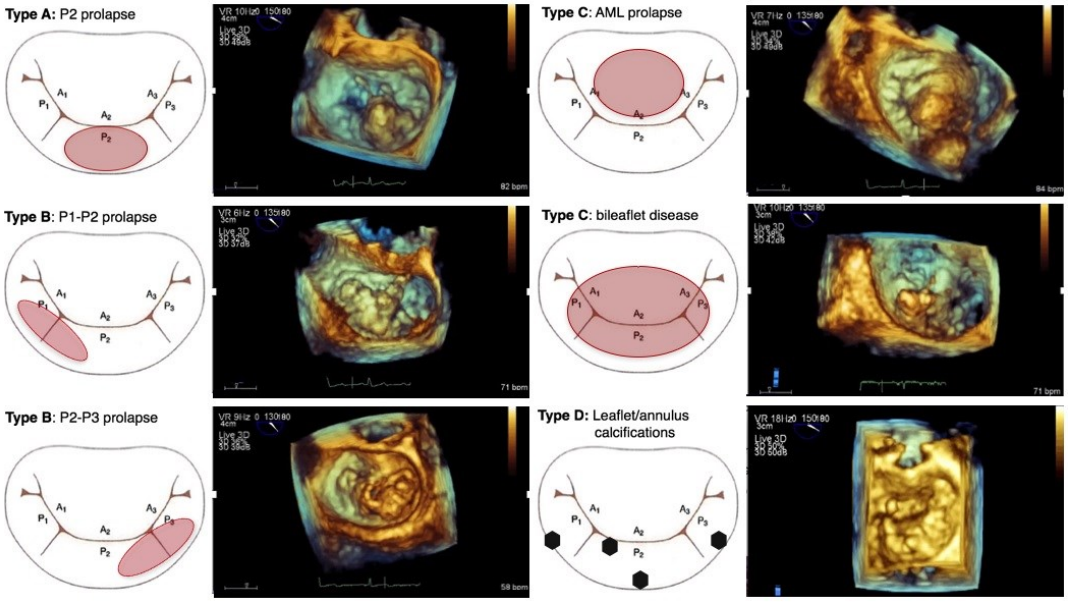

Figure 1-6 *Type classification according to MV geometry ,[16],[17], [18].*

A precise morphologic assessment is, in fact, important in order to plan correctly and select the most appropriate repair technique. Recently, the 2D and 3D intraoperative transoesophageal echocardiography are used in real time in many mini- or less-invasive surgical procedures, enhancing the rate of success. This aspect will be described with more accuracy in the next Chapter.

1.7 Reference

[1] S. C. Harb and B. P. Griffin, "Mitral Valve Disease: a Comprehensive Review," *Curr. Cardiol. Rep.*, vol. 19, no. 8, 2017.

[2] T. A. Timek and D. C. Miller, "Experimental and clinical assessment of mitral annular area and dynamics: What are we actually measuring?," *Ann. Thorac. Surg.*, vol. 72, no. 3, pp. 966–974, 2001.

[3] A. A. Degandt, P. A. Weber, H. A. Saber, and C. M. G. Duran, "Mitral Valve Basal Chordae: Comparative Anatomy and Terminology," *Ann. Thorac. Surg.*, vol. 84, no. 4, pp. 1250–1255, 2007.

[4] H. Muresian, "The clinical anatomy of the mitral valve," *Clinical Anatomy*, vol. 22, no. 1. pp. 85–98, 2009.

[5] T. M. Joudinaud *et al.*, "The papillary muscles as shock absorbers of the mitral valve complex. An experimental study," *Eur. J. Cardio-thoracic Surg.*, vol. 32, no. 1, pp. 96–101, 2007.

[6] D. Doyle, "An Introduction to Cardiovascular Physiology," *Br. J. Anaesth.*, vol. 107, no. 1, pp. 113–114, Jul. 2011.

[7] A. P. Yoganathan, Z. He, and S. Casey Jones, "Fluid Mechanics of Heart Valves," *Annu. Rev. Biomed. Eng.*, vol. 6, no. 1, pp. 331–362, 2004.

[8] K. D. Lau, "Numerical simulation of mitral valve function," 2012.

[9] W. A. Zoghbi *et al.*, "Recommendations for Evaluation of the Severity of Native Valvular Regurgitation with Two-dimensional and Doppler Echocardiography," *J. Am. Soc. Echocardiogr.*, vol. 16, no. 7, pp. 777–802, 2003.

[10] M. Horst Sievert, *Structural , Valvular , and Congenital Heart Disease*. 2015.

[11] H. Baumgartner *et al.*, "Echocardiographic Assessment of Valve Stenosis: EAE/ASE Recommendations for Clinical Practice," *J. Am. Soc. Echocardiogr.*, vol. 22, no. 1, pp. 1–23, 2009.

[12] R. A. Nishimura *et al.*, "2014 AHA/ACC guideline for the management of patients with valvular heart disease," *Circulation*, p. CIR--0000000000000031, 2014.

[13] U. Gabbay and C. Yosefy, "The underlying causes of chordae tendinae rupture: A systematic review," *Int. J. Cardiol.*, vol. 143, no. 2, pp. 113–118, 2010.

[14] A. F. Members *et al.*, "Guidelines on the management of valvular heart disease (version 2012) The Joint Task Force on the Management of Valvular Heart Disease of the European Society of Cardiology (ESC) and the European Association for Cardio-Thoracic Surgery (EACTS)," *Eur. Heart J.*, vol. 33, no. 19, pp. 2451–2496, 2012.

[15] J. G. Castillo, J. Solís, Á. González-Pinto, and D. H. Adams, "Surgical Echocardiography of the Mitral Valve," *Rev. Española Cardiol. (English Ed.*, vol. 64, no. 12, pp. 1169–1181, 2011.

[16] F. V. Adams DH, Rosenhek R, "Degenerative mitral valve regurgitation: best practice revolution," *Eur Hear. J.*, vol. 31(16), pp. 1958–66, 2010.

[17] A. Colli *et al.*, "Transapical off-pump mitral valve repair with Neochord implantation: Early clinical results," *Int. J. Cardiol.*, vol. 204, pp. 23–28, 2016.

[18] E. Manzan, "The Leaflet-to-Annulus Index: an echocardiographic predictor of outcomes in patients treated with the NeoChord repair procedure," 2017.

2 Mitral Valve Repair With NeoChord Procedure

2.1 Introduction

Mitral regurgitation (MR) is one of the most common valvular heart diseases, [1]. Severe MR lead to worsening of left ventricle (LV) function, pulmonary hypertension, atrial fibrillation, and death. The most common etiology in Western countries is degenerative MR (DMR) due to leaflet myxomatous degeneration and fibroelastic deficiency, that lead to leaflet prolapse or flail, [2], [3].

A wide varieties of standard cardiothoracic surgical approaches for MVR is available, including *i)* quadrangular or triangular leaflet resection that performs a resection of pathologic tissue including elongated or ruptured chordae; *ii)* edge-to-edge procedure that joins the free margin of the anterior and posterior leaflets at the side of the diseased portion; *iii)* chordal reconstruction thanks to polytetrafluoroethylene (PTFE) sutures that reconstruct the ruptured native chordae from the free edge of prolapsing segments to the papillary muscle and ensure a good coaptation length, often performed together with the implantation of *iv)* annuloplasty devices that reduce annular size in case of excessive annulus dilatation thanks to rigid or flexible annular device, [4].

All these On-pump, open-heart mitral valve repairs (MVR) are, at the moment, the preferred surgical treatments because of their well-documented advantages in terms of perioperative mortality, preservation of postoperative LV function, and long-term survival, [5].

However, recent studies have demonstrated superior results with techniques that preserve the anatomical parts of the disease rather than their resection, [6]. For this purpose, a variety of less invasive approaches for MVR are nowadays available [7]–[9].

Minimally invasive approaches for the mitral valve (MV) surgery have been proven to be at least as good and safe as the standard sternotomy approach, with excellent short- and long-term outcomes, [6], [9].

Among these, the Transapical Off-Pump Mitral Valve Repair with Neochord Implantaion has emergend as a promising approach for the repair of the mitral regurgitation (MR) [10], [11]. This technique consists in a transapical access procedure that, through the left ventricle apex zone, places artificial chords between the prolapsing mitral valve leaflets and apex area, in order to substitute unfunctional native chords and restore full valvular leaflets coaptation by means of a beating heart off-pump approach. The procedure is performed under a direct real time 2D and 3D transesophageal echocardiography (TEE) guidance, both

for the artificial chords implantation and for the final assessment of the restore, which consists in the proper tensioning and adjustement of the artificial chords. The entire procedure is performed using the NeoChord DS1000 System (*NeoChord,Inc., Minneapolis, Minnesota*), (see Figure 2-1).

In this chapter, we present some clinical results, recent advances, and new knowledge regarding the NeoChord procedure. The main objective of this chapter is to describe the potential of this new minimally invasive procedure and provide some details about the procedural steps in the light of the most important clinical outcomes.

2.2 NeoChord DS1000 Device System

The NeoChord DS1000 is a single-use hand-held device designed to deploy artificial chordae, typical the material suitable for being used as artificial chordae tendineae is ePTFE suture, to the mitral valve through the left ventricle while the heart is beating (*Description from IFU manual*).

By referring to Figure 2-1, this system consists of:hand-held delivery instrument (*a*) designed to load and deploy commercially available ePTFE sutures (expanded polytetrafluoroethylene sutures - *Gore-Tex suture W. L. Gore and Associates, Inc.,Flagstaff, Ariz*) through exchangeable cartridges (**b**) and a needle (*c*); a tethered leaflet verification display (*d*) that confirms the leaflet capture in the distal clamp of the device through four fibre optic lights. These lights reflect the tissue in between the device jaws; red light means there is blood (*e*), whereas white light corresponds to the leaflet tissue. When all the four light are white, the device is perfectly located for anchoring the suture, [12], [13].

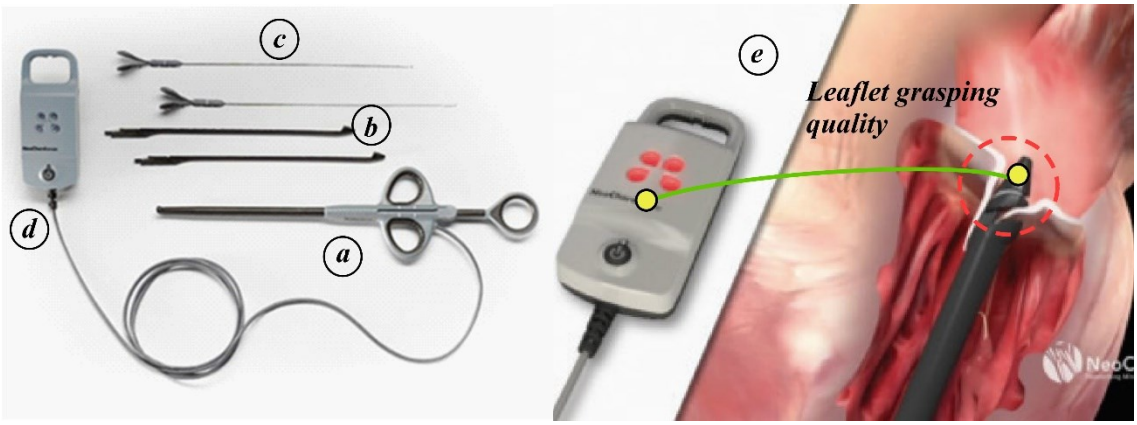

Figure 2-1 *NeoChord DS1000 consists of the hand-held delivery instrument (a), an exchangeable cartridges (b) and a needle (c), and a tethered Leaflet Verification Display (d). As the device apex grasps the leaflet, the Leaflet Verification Display gives information on leaflet grasping assessment (e), [12], [13].*

2.3 Procedural Steps

The NeoChord procedure requires the use of 2D and 3D TEE guidance. The 2D and 3D echo images are necessary during all the operative phases of the procedure, starting from the assessment of the mitral valve condition at the pre-operative phase, [14]. In particular, these images allow the analysis of the MV prolapse evaluation, the insertion of the device, the leaflet grasping and suture insertion, the tension of the suture, and, finally, the evaluation of the reduction of the MR.

All these phases are obtained with a proper echo view, able to better visualize the maneuver required. For instance, Figure 2-2 describes all the clinical steps that clinicians follow in order to confirm the success of the implant, thanks to the correct utilization of the 2D and 3D transoesophageal information, [15].

Multiplane 2D and 3D TEE (panels a, and b) allow a complete description of all segments of the valve and the proper prolapse localization. The prolapsing segments are identified during the end-systolic phase for better evaluate the leaflet displacement toward the atrium. Multi-plane imaging views (X-plane – panel c) of the mitral valve allows to observe the position of the device during the insertion. After ventriculotomy, the device is inserted in the left ventricle and then the catheter navigates toward the prolapsing segment. 3D echocardiography view is valuable for the correct leaflet grasping and assessment of leaflet capture (panel d). At this time, the surgeon has to carefully push the needle forward to pierce the valve segment. Consequently, the suture cross the valve segment and, when the needle is retracted, the suture loop together with the device are drawn back from the ventricle. The panel d, (white arrow), shows the jaws of the device and the complete capture of the leaflet. At the end of the procedure, thanks to both 2D and 3D views, the surgeons can evaluate the results of the tension of the suture. The panel e shows the reduction/disappearance of the prolapse previously shown in the panel d after the tensioning. At the end, when a satisfactory number of chordae are deployed, all the neochords are anchored to the epicardium. Finally, 3D and 2D TEE images permit to verify position, proper tension and securing of NeoChords for achieving maximal competence of the repaired valve (see panel f). For all the technical details refers to Colli et al., 2015, "*Transapical off-pump mitral valve repair with Neochord Implantation (TOP-MINI): step-by-step guide*"

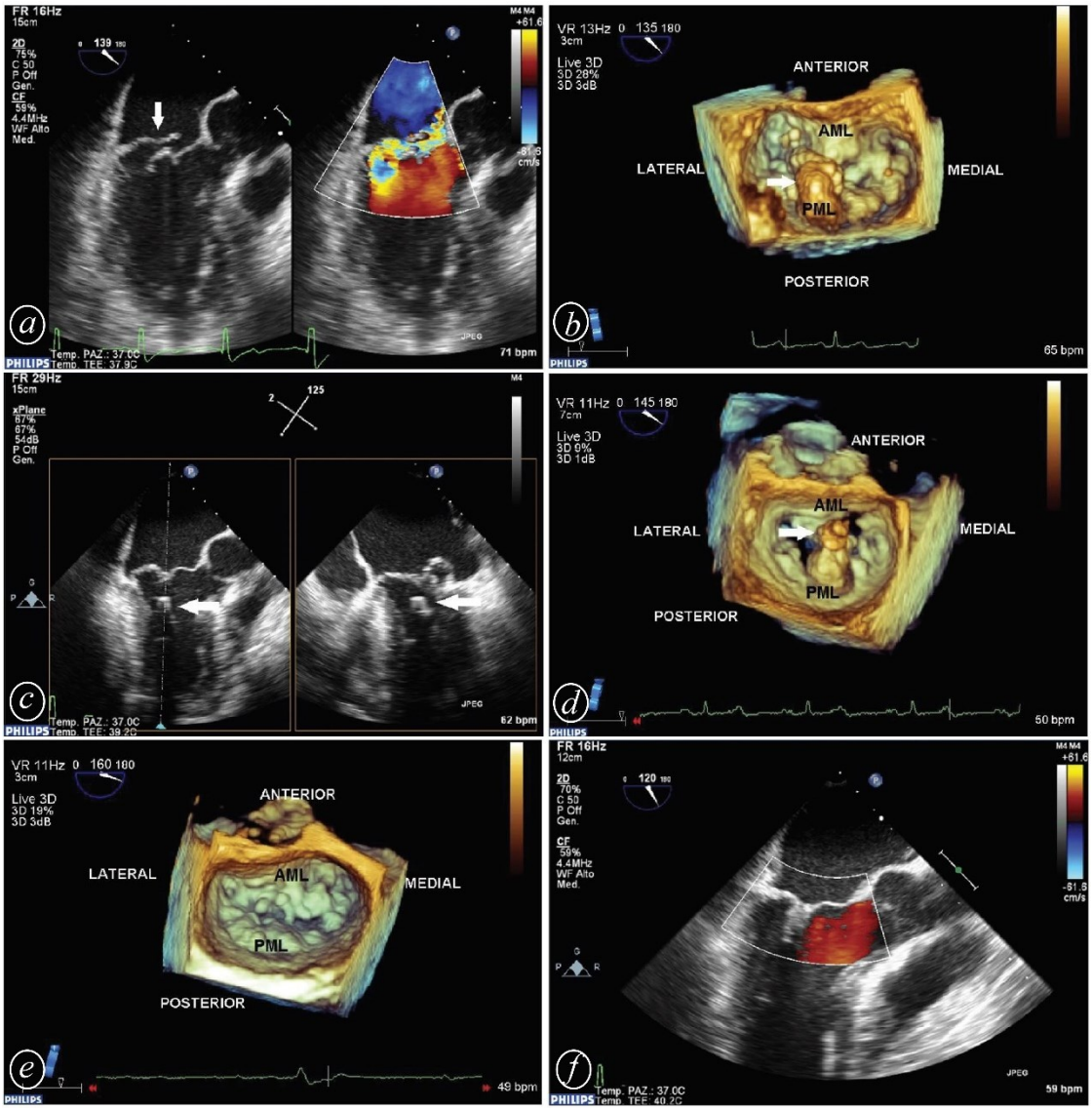

Figure 2-2 *Procedural steps under 2D and 3D TEE for NeoChord Procedure: a) 2D TEE for identification of the prolapse (arrow) in combination with the color flow Doppler that conform the regurgitation; b) 3D TEE for the assessment of mitral valve prolapse (arrow); c) multi-plane view for the visualization of the device during the insertion (arrow); d) 3D TEE for the visualization of the device during the leaflet grasping; e) 3D TEE for the evaluation of the effectiveness of the tensioning, f) 2D TEE showing no residual regurgitation after NeoChord implantation, [13]*

2.4 Clinical Outcome and potential complication

It was confirmed from initial experience of the Cardiac Surgery Unit of the Department of Cardiac, Thoracic and Vascular Science of the University of Padova (Italy), the safety and the efficacy of the minimally invasive procedure of Neochord, alternative to classical open surgical repair for the treatment of the mitral valve regurgitation. Initial results (see Figure 2-3) confirm that the efficacy of the transapical off-pump mitral valve repair is maintained during the time with a significant clinical benefit for patients, [10], [11], [16]–[19]. Clinicians of the University of Padova confirms that NeoChord procedure presents

good clinical results and can be applied to a heterogeneous population without any limitations in terms of patient risk profile.

The feasibility and reproducibility of this minimally invasive MV repair technique is proven by more than 170 patients successfully treated and followed-up since 2013. The surgeons of the Hospital of Padova, thanks to the experience acquired in this type of implant, state that the placement of two or more chords is necessary, in all the treated cases, to correctly restore the MV and significantly reduce, at least of one grade, the initial severe regurgitation. Figure 2-3 shows a published example from Colli and co-workers, about the echocardiographic outcome at follow up of the first 91 patients. The results confirm the successful rate of the procedure in terms of mitigating of the residual regurgitation.

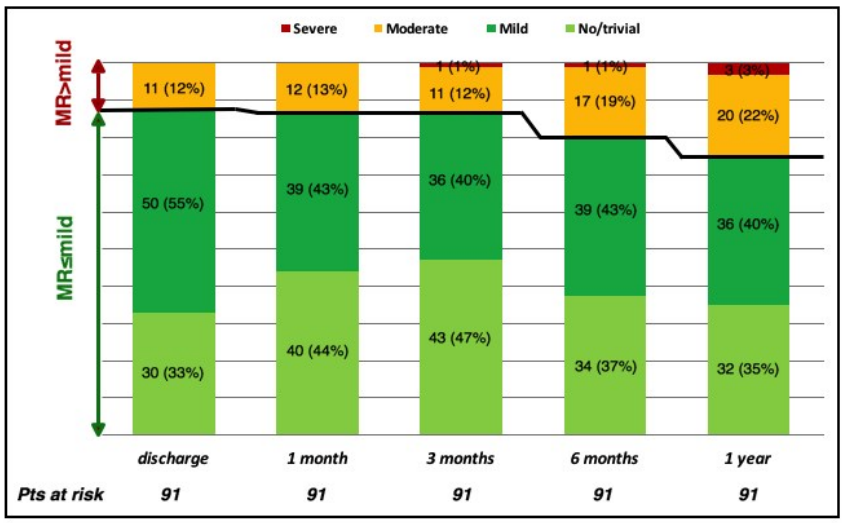

Figure 2-3 *Echocardiographic outcome at follow up. According to the grade of residual mitral regurgitation, Figure and caption from [14].*

However, during the operative stage, some adverse outcomes were also observed, such as the neochord anchoring rupture, the secondary rupture of native chordae and the relative elongation of neochords, [11].

The neochords anchoring rupture was registered mainly at the mitral leaflet stitching point, while it appears unlikely at the left ventricle muscle. In addition, this unwanted event is more frequent for sutures implanted on the anterior leaflet, rather than those implanted at the posterior leaflet. Possibly explanations are: *i)* the large size of the anterior leaflet that has to support greater pressure load in comparison to the posterior one, [20], *ii)* the unbalance of the tensioning forces that excessively increases the stress at the stitching point, and *iii)* the reduced thickness and resistance of the leaflet at the stitching points.

These issues have suggested the use of the present numerical approach to analyze firstly the mechanical stress due to the chords insertion with the aim to recognize, and possibly correct, the criticalities in the protocol of tensioning. Moreover, in order to enhance the success rate and reducing the risk in the treatment, a second aspect related to the role of ventricular entry sites has caught our attention, [21], [22].

The native chordae rupture is the consequence of the crossing between native and artificial chords that leads to a constant scratching and, at mid-long term, the deterioration of the original chordae. This unwanted impact is a result of a surgical technical error, which can be overcome by acquiring a large experience in the procedure, as well as, thanks to the improving of the imaging-guided protocol (TEE and CT). This issue is related to the analysis of the suture's trajectories during the implant due to the possible change of the ventricular entry site. The uncertain is due to the impossibility, at this time, to observe the native chordae structures from the clinical images (3D TEE), but some preliminary results in terms of interactions among sutures and mitral valve sub-structures were found thanks to the numerical approach here presented.

NeoChords relative elongation was observed as a result of early LV remodeling and LV volume reduction after the implant. This is due to the more physiological ventricle working condition, resulting from the reduction of the mitral regurge. The final suture's length is then longer to maintain the proper position of the prolapsed leaflet, causing a decreasing of the effectiveness of the restore, and, when the volume reduction is consistent, it can lead to the inactivation of the implanted sutures. For this reason, a slight over-tension of the sutures is always applied during the NeoChord final fixation, [12].

2.5 Development of the procedure

For improving the efficacy of the NeoChord technique some aspects of the procedure have been standardized, e.g., the patient selection criteria, the ventricular access site location, the transesophageal echocardiography guidance protocol and CT analysis, and the neochordae tensioning protocol.

The patient selection criteria are based on the analysis of clinical images, i.e., echo and CT, routinely used for the clinical assessment of a cardiac pathology, [23]. The imaging, indeed, allows to correctly classified the anatomical features of the MV diseases, and, according to Colli and co-workers, the NeoChord procedure can be safely adopted to treat the patients affected by specific prolapsed MV, recognized as *i)* isolated posterior prolapse or flail located in the P2 segment (Type A prolapse), *ii)* extensive posterior prolapse that

involves multi-segment, i.e., non- symmetric posterior prolapse (P1-P2; P2-P3 segments – Type B prolapse), *iii)* extensive anterior prolapse or bileaflet disease (Type C prolapse) and, *iv)* posterior prolapse in combination of annulus calcifications (Type D prolapse).

In addition, a new parameter, the so-called LAI (*leaflet-to-annulus index*, defined as the sum of the anterior and posterior length divide by the antero-posterior annulus dimension), was recently introduced to evaluate the patient suitability for being treated by the NeoChord implantation, [24]. This index is related to the overlapping between leaflets and predicts the appropriate level of coaptation after the NeoChord repair. Recent works of Colli and co-workers demonstrated that LAI greater than 1.25 in restored MV is a strong predictor of less than mild MR at 1 year of follow-up. In addition, it was demonstrated that, if the LAI is less than the established 1.25 threshold, a patient could, however, benefit from the NeoChord implant just providing few modifications at the procedures, with the aim to increase the potential MV leaflet coaptation by changing the neochords trajectories. This occurrence was developed on the basis of a study focused on the selection of the best ventricular access site in order to improve the postoperative coaptation length, [22]. According to Colli and co-workers, the clinical analysis has suggested that patients with low LAI index can benefit from a more anterior working angle, since it increases the postprocedure LAI, and thus the effectiveness of the procedure, more than an implant carried out by the standard posterior access.

In addition to the standard echocardiography techniques, also, the use of CT scan has permitted an advance in terms of NeoChord safety repair, since it provides, with a good accuracy, details of the cardiac anatomy. Such information are fundamental to analyse all the critical possible interference of the device with the native subvalvular apparatus and to overcome some critical technical aspects of the procedure, in patients presenting abnormal MV apparatus, i.e., native chordae rupture, safety navigation of the device across the left ventricle, [11], [25].

Currently, the clinical protocol lacks information about the modality of chords tensioning and transfers to the surgeons this operative choice. Usually, the artificial sutures are pulled following two different scheme. In the first case, the surgeons prefer pulled at the same time the strands in order to guarantee a uniform tensioning on the leaflet; whereas, in the second case, the surgeons pull the strands one at a time, enhancing in this way the accuracy of the leaflet repositioning. Both the schemes have provided good clinical results, but some concerns about their safety and actual efficacy need to be addressed, such as the additional leaflet stress transmission due to the stitching in addition to the amount of final overlap

between anterior and posterior leaflets. Moreover, as previously said, the proper entry site position for the identification of the best trajectories to be assigned to the neochords is an issue, which deserves specific investigations, also in light of potential new devices expected on the market to treat, through artificial chords, the MV diseases.

Future perspective for the optimization of the procedure here presented can be found thanks to the use of numerical simulations, which allow to assess and identify the proper design of the implant.

The presented thesis work is developed with this particular aim. We want to identify the most suitable implantation protocol and access site localization and analyze through an engineering approach the commonly reported procedural complications that are pointed out during these years of clinical experience.

2.6 References

[1] B. Iung *et al.*, "A prospective survey of patients with valvular heart disease in Europe: The Euro Heart Survey on valvular heart disease," *Eur. Heart J.*, vol. 24, no. 13, pp. 1231–1243, 2003.

[2] R. A. Nishimura *et al.*, "2014 AHA/ACC guideline for the management of patients with valvular heart disease," *Circulation*, p. CIR--0000000000000031, 2014.

[3] A. Vahanian *et al.*, "Guidelines on the management of valvular heart disease (version 2012)," *Eur. Heart J.*, vol. 33, no. 19, pp. 2451–2496, 2012.

[4] A. Madesis *et al.*, "Review of mitral valve insufficiency: Repair or replacement," *J. Thorac. Dis.*, vol. 6, no. SUPPL1, 2014.

[5] R. M. Suri *et al.*, "Association between early surgical intervention vs watchful waiting and outcomes for mitral regurgitation due to flail mitral valve leaflets," *JAMA - J. Am. Med. Assoc.*, vol. 310, no. 6, pp. 609–616, 2013.

[6] P. Perier *et al.*, "Toward a new paradigm for the reconstruction of posterior leaflet prolapse: midterm results of the 'respect rather than resect' approach," *Ann. Thorac. Surg.*, vol. 86, no. 3, pp. 718–725, 2008.

[7] S. Kuwata, M. Taramasso, A. Guidotti, F. Nietlispach, and F. Maisano, "Ongoing and future directions in percutaneous treatment of mitral regurgitation," *Expert Rev. Cardiovasc. Ther.*, vol. 15, no. 6, pp. 441–446, Jun. 2017.

[8] L. Testa, A. Latib, R. A. Montone, and F. Bedogni, "Transcatheter mitral valve regurgitation treatment: State of the art and a glimpse to the future," *J. Thorac. Cardiovasc. Surg.*, vol. 152, no. 2, pp. 319–327, 2016.

[9] T. Feldman and A. Young, "Percutaneous approaches to valve repair for mitral regurgitation," *J. Am. Coll. Cardiol.*, vol. 63, no. 20, pp. 2057–2068, 2014.

[10] G. Gerosa, A. D'Onofrio, L. Besola, and A. Colli, "Transoesophageal echo-guided mitral valve repair using the Harpoon system," *Eur. J. Cardio-Thoracic Surg.*, vol. 00, no. January, pp. 1–3, 2017.

[11] A. Colli *et al.*, "Transapical off-pump mitral valve repair with Neochord Implantation (TOP-MINI): step-by-step guide," *Ann. Cardiothorac. Surg.*, vol. 4, no. 3, p. 295, 2015.

[12] A. Colli, R. Bellu, D. Pittarello, and G. Gerosa, "Transapical off-pump Neochord implantation on bileaflet prolapse to treat severe mitral regurgitation," *Interact. Cardiovasc. Thorac. Surg.*, p. ivv192, 2015.

[13] A. Colli *et al.*, "Transcatheter Chordal Repair for Degenerative Mitral Regurgitation," *Card. Interv. Today*, vol. 12, no. 4, pp. 45–49, 2018.

[14] P. Demetrio, C. Andrea, F. Gianclaudio, M. Antonio, G. Gino, and O. Carlo, "Transesophageal echocardiography in NeoChord procedure.," *Ann. Card. Anaesth.*, vol. 18, no. 2, pp. 191–197, 2015.

[15] E. Manzan, "The Leaflet-to-Annulus Index: an echocardiographic predictor of outcomes in patients treated with the NeoChord repair procedure," 2017.

[16] A. Colli *et al.*, "Transapical off-pump mitral valve repair with Neochord implantation: Early clinical results," *Int. J. Cardiol.*, vol. 204, pp. 23–28, 2016.

[17] A. Colli *et al.*, "TEE-guided transapical beating-heart neochord implantation in mitral regurgitation," *JACC Cardiovasc. Imaging*, vol. 7, no. 3, pp. 322–323, 2014.

[18] J. Seeburger *et al.*, "Trans-apical beating-heart implantation of neo-chordae to mitral valve leaflets: Results of an acute animal study," *Eur. J. Cardio-thoracic Surg.*, vol. 41, no. 1, pp. 173–176, 2012.

[19] J. Seeburger *et al.*, "Off-pump transapical implantation of artificial neo-chordae to correct mitral regurgitation: The tact trial (transapical artificial chordae tendinae) proof of concept," *J. Am. Coll. Cardiol.*, vol. 63, no. 9, pp. 914–919, 2014.

[20] H. Jensen *et al.*, "Transapical neochord implantation: Is tension of artificial chordae tendineae dependent on the insertion site?," *J. Thorac. Cardiovasc. Surg.*, vol. 148, no. 1, pp. 138–143, 2014.

[21] A. Colli *et al.*, "CT for the Transapical Off-Pump Mitral Valve Repair With Neochord Implantation Procedure," *JACC Cardiovasc. Imaging*, vol. 10, no. 11, pp. 1397–1400, 2017.

[22] A. Colli *et al.*, "Patient-Specific Ventricular Access Site Selection for the NeoChord Mitral Valve Repair Procedure," *Ann. Thorac. Surg.*, vol. 104, no. 2, pp. e199–e202, 2017.

[23] M. Horst Sievert, *Structural , Valvular , and Congenital Heart Disease*. 2015.

[24] A. Colli *et al.*, "the Importance of the Leaflet-To-Annular Mismatch Index for Patients Undergoing Echo Guided Transapical Off-Pump Mitral Valve Repair With Neochord Implantation," *J. Am. Coll. Cardiol.*, vol. 67, no. 13, p. 1792, 2016.

[25] A. Colli, E. Manzan, F. Zucchetta, C. Sarais, D. Pittarello, and G. Gerosa, "Feasibility of anterior mitral leaflet flail repair with transapical beating-heart neochord implantation," *JACC Cardiovasc. Interv.*, vol. 7, no. 11, pp. 1320–1321, 2014.

3 Mitral Valve Model and Simulations: Tensioning Protocols for NeoChord Procedure

3.1 Introduction

Numerical investigations are nowadays largely used to assess the safety and efficacy of cardiovascular devices and procedures, by identifying an enhanced medical practice and support clinical decisions, [1]–[4], [5]. For this reason, a number of *in-silico* studies have attempted to investigate the biomechanics of MV repair with neo-chords implantation, performed in a classical open-chest approach, [6]–[8], analyzing the post-implant configuration after the complete surgical procedure. In this section, we present recent results about numerical optimization of the NeoChord procedure, that differently by the cited studies is performed in beating-heart approach.

We investigated, by means of numerical simulations, a critical aspect of this new minimally invasive treatment for the repair of the mitral valve (MV) prolapse: *the tensioning protocol for the final fixation of the artificial sutures implanted*. A first simplify MV model, able to reproduce the complete MV apparatus and the main characteristic of the artificial implant, was developed. In particular, the study focused on the main characteristics of the geometrical model, i.e., size, 3D MV design, Virtual repaired model, and all the important aspects necessary for properly simulating the dynamics of the neochords implant, i.e., boundary condition (BC), pressure condition, tensioning simulation. In the final part of the chapter, we present and comment all the results in terms of MV restoration, i.e., the contact area and the reduction of the prolapse, and the final pro and cons of the tensioning protocol investigated in terms of final stresses and tensioning forces.

3.2 The tensioning protocols investigated (AT and 1by1)

Transapical off-pump mitral valve repair with neochord implantation (NeoChord Procedure) is an established technique for mini-invasive intervention on mitral valve prolapse/flail. As seen before, the procedure involves the positioning of artificial chords, whose length/tension is adjusted intraoperatively, adopting different methods based on the experience of the surgeon. This unsystematic approach occasionally leads to complications, such as leaflet rupture and excessive/insufficient load on the neochords, [9]. In this first study, a finite element model of a generalized prolapsing mitral valve is used to verify the effect of two alternative tensioning approaches: the '***all together (AT)***' strategy, i.e. all chords are tensioned contemporarily all at once, and the '***one by one (1by1)***', i.e. the chords

are tensioned one at a time, following a certain order, by subsequently applying to each chord a proper tensioning.

For the 1by1 approach, in order to examine the different strategies commonly adopted by surgeons when repairing MV prolapse by NeoChord procedure, the following possible sequences of chord pulling were simulated (see Figure 3-1):

- central to lateral pulling (1by1a);
- lateral to central (1by1b);
- lateral to lateral (1by1c).

For both tensioning strategies and sequences, the intraoperative leaflets coaptation, the stress distribution in the valve apparatus, and the tensioning force in each chord are determined by means of numerical simulations of a generalized MV prolapse; specifically, we considered a P2 prolapse.

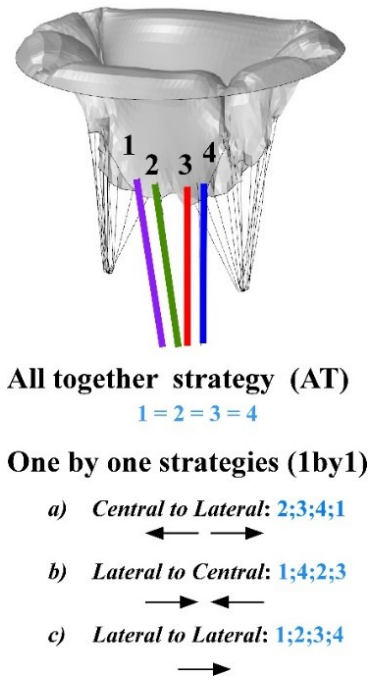

Figure 3-1 *Simulated protocol tensioning. In AT procedure all neochords are pulled together. In the 1by1 procedure the chords are pulled one by one following three sequences: a) central to lateral, b) lateral to central, and c) lateral to lateral. In all simulations, neochords are numbered in crescent order starting from the left external position to the right external position.*

3.3 Mitral Valve Model

3.3.1 Geometry

Unless affected by diseases, the MV prevents blood backflow from the left ventricle to atrium during systole by coaptation of posterior and anterior leaflets; a number of tendinous strings (chordae tendinae) contribute to holding the closed valve in place, by tethering the

leaflets to the ventricular wall via papillary muscles structure. As described in Chapter 1, the MV presents a complex structure with a large population variability in both anatomy (e.g. the number of chordae, leaflets, and annulus shape) and size.

Hence, in order to generalize the results, in this first part of thesis work, a first numerical study about NeoChord tensioning was developed, with a geometrical model considering an ideal average morphology and size for all fundamental elements of the valvular apparatus [10]. The leaflet and annulus shapes and the native chordae tree distribution adopted are shown in Figure 3-2. All main parameters of the valve geometry, e.g. the thickness and cross-sectional area used for the leaflets and chordae in the various portions of the model, are summarized in Table 3-1.

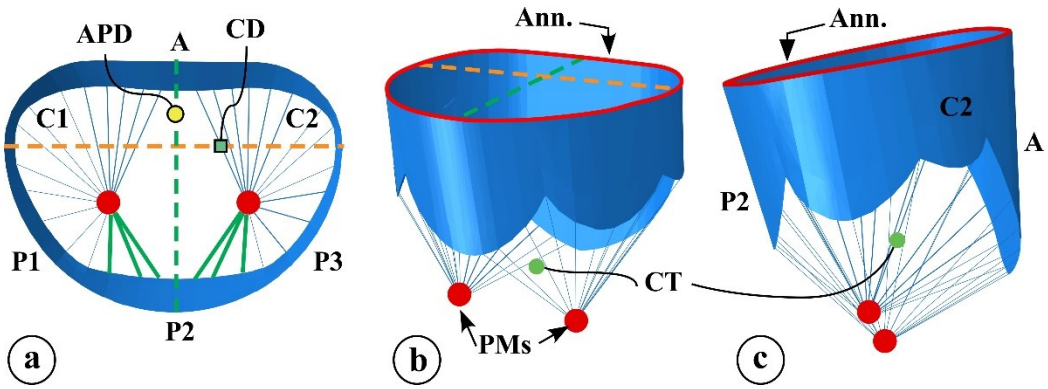

Figure 3-2 *MV geometry of the model at the end of diastole. a) Atrial to ventricle view: A indicates the anterior leaflet, C1 and C2 the commissural leaflet scallops, P1, P2 and P3 the posterior leaflet scallops, and APD and CD the ateropostirial and commissures distance, respectively. b) Perspective view: red lines indicates MV annulus. CT the chordae tendinae, and PMs the papillary muscles. c) Lateral view. The chordae tendinae in green have been cut off to generate prolapse.*

Table 3-1 *Dimensional parameters adopted for leaflets and chordae of the MV model. Data were set in accordance with Lau et al., [2] and Rim et al., [4]. APD and CD indicate the ateropostirial and commissures distance, respectively.*

	Leaflets			
	Anterior	Posterior		Commissure
		P2	P1/P3	
Height (mm)	20	13.8	11.2	8.8
Ann. Lenght (mm)	32.3	17.5	12.7	6.7
Area (mm^2)	457.6	204.4	123.9	51.2
Thickness (mm)	0.69	0.51		0.6
Chordae Tendineae				
Cross-sectional area (mm^2)	0.29	0.27		0.28
Annulus				
APD (mm)	22			
CD (mm)	30			
Area (mm^2)	552.7			

The leaflets were designed to include the common anatomical segments usually identified, including the anterior leaflet scallop, ***A***; the commissural leaflet scallops, ***C1*** and ***C2***; the posterior leaflet scallops ***P1***, ***P2***, and ***P3***. The model presents a perfect flat D-shape according to a previous work of Kunzelman et al., [11] and Lau, [10] and an idealized representation of the papillary muscles, as a simple anchoring site for all the chordae distribution.

3.3.2 Virtual Repaired Model

A MV incompetence was then simulated by detaching six central chords (see green chords in Figure 3-2), leading to a central width prolapse that is the most common leaflet disease for patients who underwent NeoChord repair, [12].

In the prolapsed scenario, the repair was simulated by adding four artificial neochords between the margin of the prolapsed leaflets portion and the ventricle entry site (see Figure 3-3), [13]. The entry site was located 40 mm apart from the annulus, according to in-vivo measurements, to form the optimal neochord trajectory of implantation, [14].

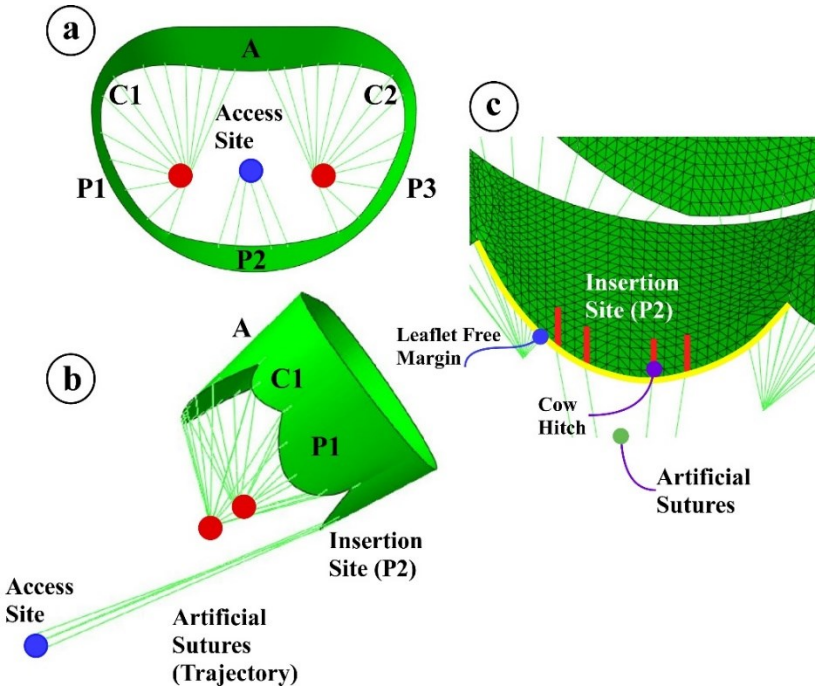

Figure 3-3 *Geometrical representation of the virtual repair: a) surgical view of the MV geometry, the blue circle identify the posterior access site located between the PMs; b) lateral view of the virtual repair. It is possible to observe the posterior 3D trajectory of the sutures; c) particular of the insertion site. The four artificial chordae substitute the native chordae eliminated for the simulation of the prolapse in the P2 segment of the posterior leaflet.*

Figure 3-3 shows the reference MV geometry with the virtual implantation of the artificial sutures. Specifically, four chords were implanted to simulate the valve restoration in according to the clinical practice [15], where this type of prolapse (central posterior prolapse - Type A, [16]) is commonly treated with the same number of sutures.

The panels, a, and b of Figure 3-3 show the 3D position of the insertion site (leaflet insertion site) and the assess site (apex access site). The former is defined by the entire P2 segment of the posterior leaflet, where all the sutures following the free margin (yellow line. –Figure 3-3, panel c) were positioned.

The access site (blue circle, Figure 3-3, a-b), positioned around the ventricular apex zone, identifies the so-called "*posterior access site*", [14]. Its position, located in the posterior left ventricle wall, defines the entry site centered between the papillary muscles. This is the preferred choice for the repair of the central prolapse of the posterior leaflet, [17]. The trajectory that derives from this access position, allows to implant the sutures without interference with the native chordae structure and the anterior leaflet, as well. The effect of the ventricular access site selection will be investigated in the next chapter, focusing on the effects of a different working angle of the sutures and, consequently, on the location of the entry site.

3.4 Mechanical Characterization

3.4.1 Leaflets

The mechanics of the leaflets under tension is non–linear and anisotropic. The non–linearity is derived by an internal microstructural arrangement of elastin and collagen fibers. Three distinct layers for dimension and structures characterize each leaflet, namely, Atrialis, Fibrosa, and Ventricularis, [18]. In general, the anterior leaflet shows ticker layers and consequently, it is stiffer than the posterior leaflet. On the other hand, the observed non linearity mainly depends on the fibers arrangement; indeed, both leaflets show a space-variable fiber orientation that locally alter the elastic response of the leaflet isotropic matrix, [19], as shown in Figure 3-4, where the mechanical response of the mitral valve, [20], has been characterized in the circumferential and directions. Bi-axial tests on porcine valves, performed by Newman, [20], have shown that the leaflets are stiffer in the circumferential directions, as is possible observe in Figure 3-4 at the red/black and blue/green lines, respectively. The posterior leaflet results more isotropic and more extensible than the anterior leaflet.

Despite these differences, since the purpose of the present analysis aims at recognizing the peculiarities of the neochord implant in a simplest MV model, in our study, we assume that the leaflet material is elastic and isotropic. The leaflets were modeled as membranes, with an isotropic hyperelastic incompressible constitutive law based on a 5th order reduced polynomial strain energy potential formulation, $\boldsymbol{U}$, that reads:

$$U = \sum_{i=1}^{5} C_i(\bar{I}_1 - 3) + \frac{1}{D_1}(J_{el} - 1)^2 \qquad (1)$$

Where $\boldsymbol{I_1}$ is the first strain invariant, $\boldsymbol{j_{el}}$ is the elastic volume strain and $\boldsymbol{C_i}$ and $\boldsymbol{D_1}$ are the coefficients determined from mechanical tests performed on porcine mitral valves by May-Newman and Yin, [20], averaging the data obtained along radial and circumferential direction, and summarized in Table 3-2. As anticipate before, the strain-stress behavior obtained by original biaxial mechanical tests and the averaged results are shown in Figure 3-4. The solid lines represent the stress-strain behavior in the radial and circumferential direction (red/black and blue/green lines) and for the anterior and posterior leaflets, respectively. The dotted orange and blue lines represent the average stress-strain relationship for the anterior and posterior leaflet, respectively. These averaged curves were implemented into the material model for the simulations.

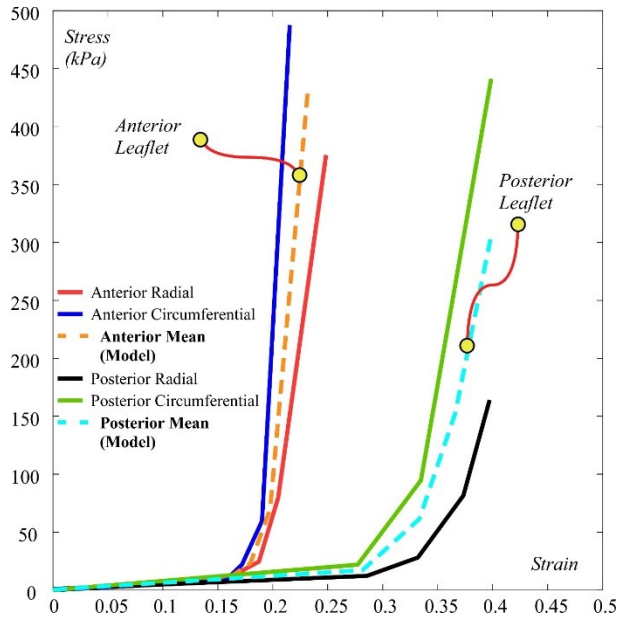

Figure 3-4 *Stress-Strain behavior. Solid lines represents the mechanical tests performed on porcine mitral valves by May-Newman and Yin, [11]. Dotted lines represents the averaged curves obtained between*

radial and circumferential behavior. The behavior between the anterior and posterior leaflet was distinguished.

Table 3-2 *Determined coefficients of equation (1) for anterior and posterior leaflets*

	D_1	C_{10}	C_{20}	C_{30}	C_{40}	C_{50}
Anterior leaflet	0.78	0.05	-0.36	1.64	-4.38	5.18
Posterior leaflet	0.47	0.09	-0.06	-0.11	0.15	-3.47

3.4.2 Native Chordae and Artificial Suture

The chordae tendineae are composed of a mixture of collagen and elastin [Ref. 65]. The structure of the chordae presents collagen fibers in the center of the chordae, aligned with the axis direction. The Chordal structure exhibits a non–linear stress-strain response. For the determination of the biomechanical response, since chordal fiber are aligned along the main direction, was performed the uniaxial tensile test by Kunzelman and co-workers, [Ref. 67]. These test was performed for different chordal type, i.e., marginal and basal, and the results indicates that the marginal chordae are less extensible and stiffer than the basal chordae.

For simplicity, Native Chordae in the present analysis were modeled as linear elastic trusses, with Young modulus ***E*** equal to 40 MPa, as suggested by previous investigations [10], [21].

In the neochord procedure, artificial chords are usually made by e-PTFE CV-4 Gore-Tex sutures with a cross-section of 0.074 mm^2, tied to the leaflet margin with a girth hitch knot approach, resulting in two suture stands pulled in the same direction [13]. In the model, each artificial chord was represented by linear truss element with a circular cross-section of 0.148 mm^2 , i.e. equal to the sum of the cross-section of the two strands. The neochord's Young modulus was determined experimentally by performing tension testing on an e-PTFE wire. For the test, the wire was settled on the tensile testing machine (Zwick-Roll, Zwick GmbH & Co.KG, Zwick USA) in a wet environment of saline solution at a temperature of 37°C, in order to recreate physiological conditions (see Figure 3-5). A 40 mm initial length (l_o) was used, i.e. the length of the neochords in the numerical model. Figure 3-6 shows the results of the tensile tests; linear fitting of data is also reported, indicating an average value of the Young Modulus equal to 2.3 GPa.

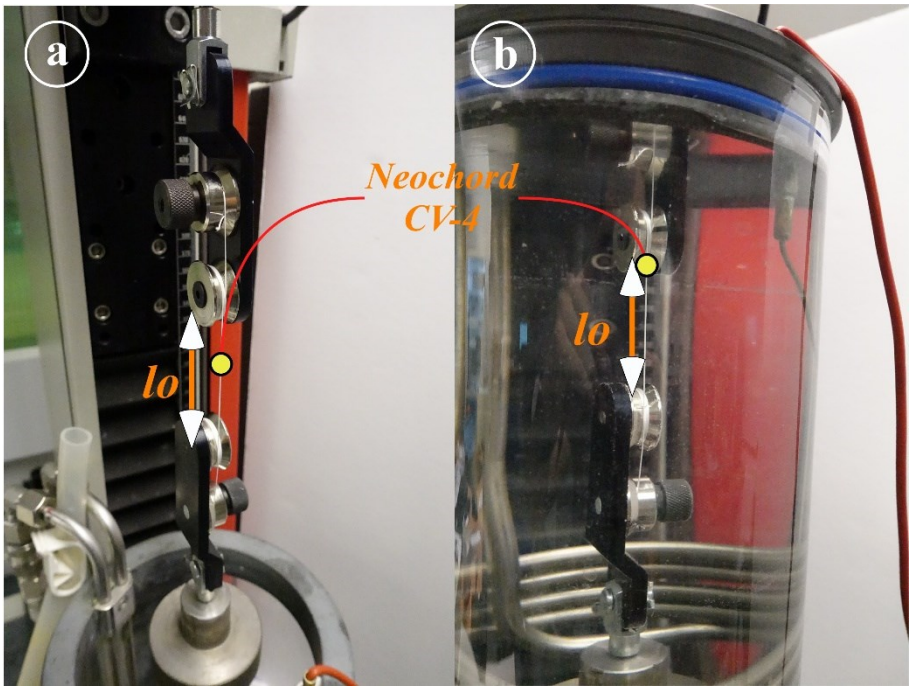

Figure 3-5 *Experimental set-up for the evaluation of the mechanical characteristics of the suture wire used for the NeoChord procedure (CV-4 Gore-Tex suture). Panel a) preparation of the wire and set the initial length lo equal to 40 mm. Panel b) position of the wire inside a saline solution at 37°C. The entire test was performed inside a wet environmental to recreating physiological condition.*

3.4.3 Determination of Young's modulus of neochords sutures

In this subsection is reported a sensitivity analysis about the definition of the mechanical characteristics of the artificial sutures. In particular, preliminary numerical simulations were performed in order to understand the relevance of the elastic modulus, ***E***, to assign to the artificial sutures. All the results here presented are explained with more detailed in the result section of this chapter.

Since the number of experimental runs did not allow a robust statistical analysis to estimate the Young Modulus variability, we performed a numerical sensitivity study to investigate Young Modulus effect on the overall results of the simulations. A comparative analysis of the tension force on the chords, contact area, and maximum stress on the leaflet P2 was performed by varying ***E*** from 0.5 to 5.0 GPa, by applying in all tests the AT tensioning. The results presented in Figure 3-7 show small differences in both neochordal forces and contact area (panel a, and b), and maximum leaflet stress variation lower than 10% (panel c), highlighting only a weakly dependence of the outcomes on the mechanical properties of the sutures. For this reason, we chose for all simulations the calculated value of 2.3 GPa being aware that small variation of this value affects negligibly the final results.

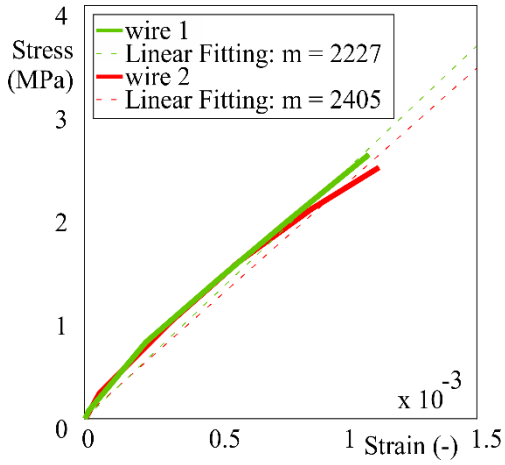

Figure 3-6 Experimental results of single tensile tests of Neochord suture wires (solid lines) and basic liner fitting (dotted lines). The angular coefficient E represents the Young's Modulus of the e-PTFE wires.

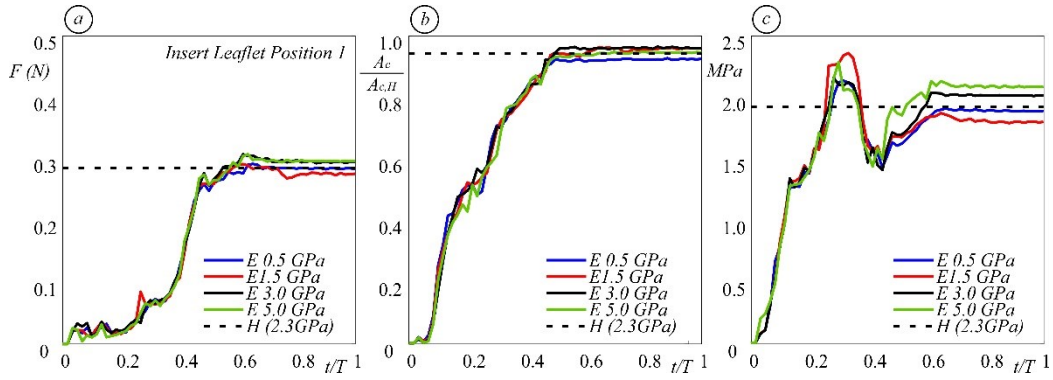

Figure 3-7 *Sensitivity numerical analysis results in terms of the chordal force (panel a), contact area (panel b) and maximum stress on the P2 leaflet (panel c). The analysis was performed changing the stiffness of the suture in a range of between 0.5 to 5.0 GPa and the results were compared with the reference value given by the healthy configuration H (dotted lines).*

3.5 Numerical Simulations

The mitral valve was modeled by using the explicit approach provided by the finite element code ABAQUS (*SIMULIA, Providence, RI*). The Leaflets and both the chords, native and artificial, were represented by linear triangular membrane elements (2D elements – M3D3, 3 nodes triangular membrane) and truss (1D elements – T3D2, 2 nodes linear 3D truss), respectively.

3.5.1 Merge of the elements (leaflets and chordae)

The connections between the leaflets free-margin and the chordae tendineae were modeled simulating the physiological intra-leaflets insertion of the native chords as described by Muresian,[22], on the basis of an accurate clinical analysis. In the model, along with the free-margin insertion, the native chordae elements were prolonged inside the

leaflets by sharing three nodes, thus avoiding unrealistic stress concentration and singularity points (see Figure 3-8, panel c).

As described before, the pierced between the leaflet and artificial suture is done with a girth hitch knot approach. For the aim of this work is not properly simulated this connection, but the link was simulated with the same approach used for connecting the leaflets free margin and native chordae. For this reason, the artificial sutures were prolonged inside the leaflet (P2 segment) for five nodes, reaching a length of about 4 mm. (see Figure 3-8, panel b).

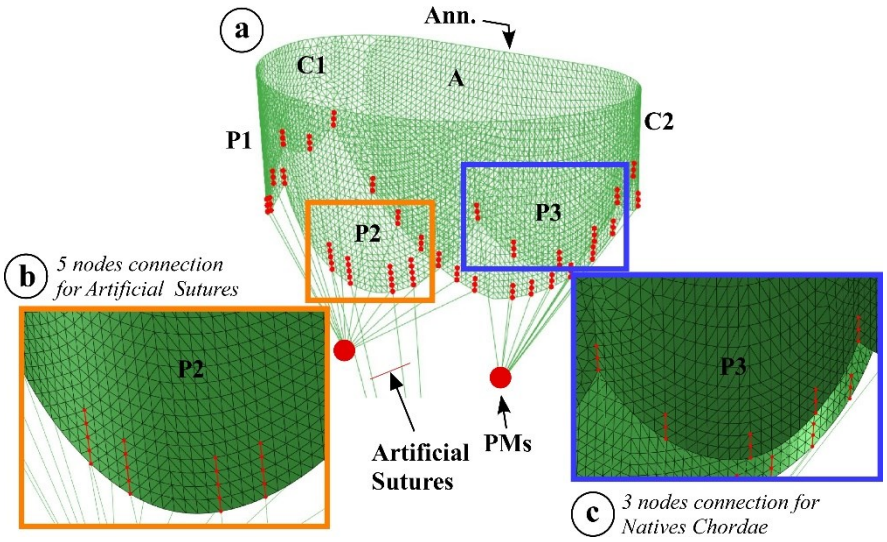

Figure 3-8 *Leaflets and chordae connection: a) MV in the fully open configuration (end-diastolic phase), the nodes share among leaflets and both type of chordae (Native and artificial); b) particular of the link, made of 5 nodes, between P2 segment and the four sutures implanted, c) particular of the connection between leaflet and native chordae. The connection is repeated equal for all the attached points. The nodes share among leaflets and both types of chordae are highlighted in red.*

3.5.2 Boundary Condition: Annulus and Papillary Muscle

As previously describe, in the physiological dynamic of the MV, annular valve dimension and shape, and papillary muscle position varies during the cardiac cycle. Since the proposed study is concerned essentially with the systolic phase, in this simplified mitral valve model the dynamic motion of the annulus and papillary muscles were not simulated. For this reason, we kept fixed the annular profile and maintained a constant distance between the annulus plane and the papillary muscles (see Figure 3-9). These assumptions, which are common in the literature [10], [11], are considered acceptable due to the comparative nature of this study.

The nodes describing the annulus were fixed in space, allowing rotations of the leaflets elements about all axes. Similarly, the chordae were pinned at the nodes corresponding to

the papillary muscles. Figure 3-9, panel a, shows the hinge condition imposed to both annuls profile and PMs tips.

3.5.3 Load Condition: Comparison between pulsatile and steady pressure condition

Figure 3-9 describes all the necessary steps to simulating the MV closure. The pictures shows the closure phase of the reference model without the simulation of the neochord implant. The reference model includes all the native chordae in order to ensure the proper closure of the MV, and it was used in the numerical analysis to estimate the optimal anterior-posterior leaflets coaptation achievable with the selected MV description (Figure 3-9, panel d).

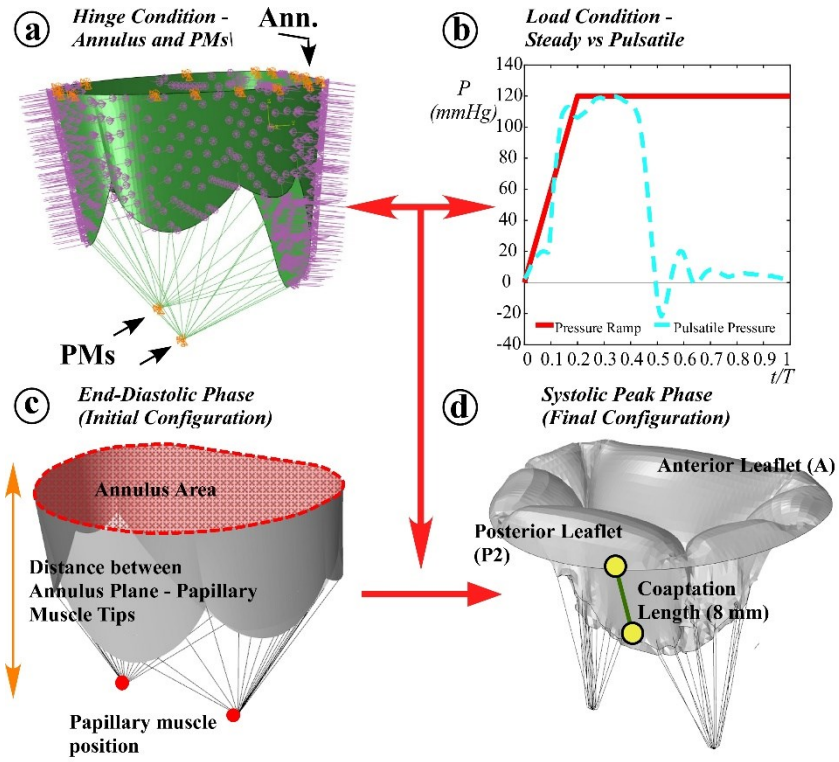

Figure 3-9 *Boundary and Load Condition: a) Hinge Condition (yellow dots) and uniform pressure on the ventricular side of the leaflets; b) End-diastole configuration (initial configuration); c) plot of the pressure condition assigned, d) closed valve configuration of the healthy MV configuration.*

The dynamic load condition is described as a pressure applied uniformly to the ventricular surface of the leaflets. Preliminarily, we tested the model both in quasi-steady and pulsatile condition (red and blue light lines, respectively – Figure 3-9, panel b). The panel c shows the initial configuration at the beginning of the simulation, i.e. the unloaded valve model in a fully open position, [2]. Thanks to the pressure conditions previously mentioned, the simulation describes the closure phase indicated in the panel d of Figure 3-9.

Since the model does not describe the annulus and papillary muscles dynamics occurring during the cardiac cycle, some preliminary simulations were performed to verify the effect of the load history on the systolic configuration. In particular, the comparison between the values of the maximum principal stresses at the peak load (Figure 3-10, panel d, green dot, top), which were obtained applying physiologically pulsatile pressures and steady pressure conditions reached by ramping the load linearly (Figure 3-10, panel d), indicated lower stress in pulsatile condition, with differences inferior to 10%. Differences in term of displacement were negligible and inferior to 0.5%, (see Figure 3-10, panel d, bottom).

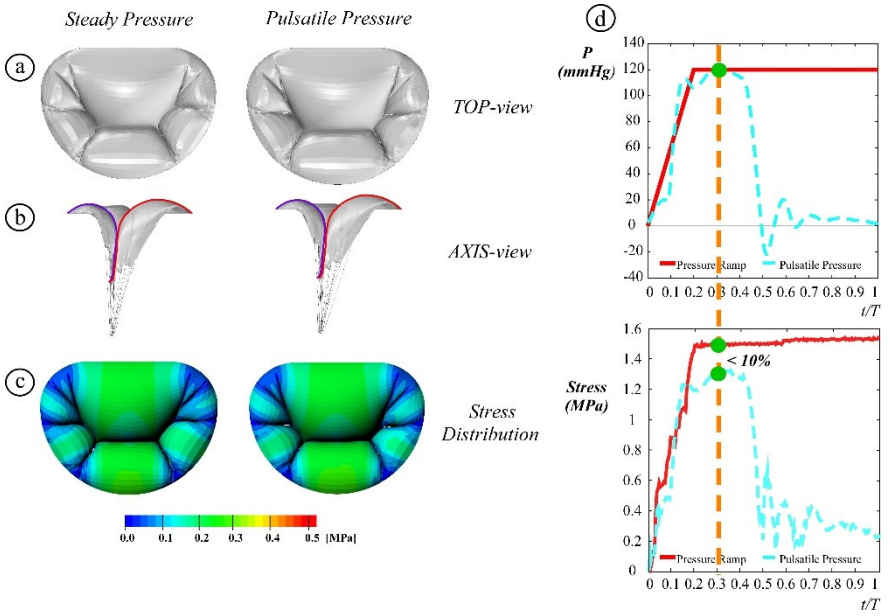

Figure 3-10 *Comparison in terms of the leaflets maximum principal stress and displacements of the history load condition (application of a constant pressure vs physiological pressure condition): a) top-view of the MV; qualitative closure phase, b) axis view at the closure phase, c) stress pattern distribution at the systolic peak; d) comparison of the maximum stress at the systolic peck for both pressure condition imposed.*

Hence, the decision was taken to apply a spatially uniform pressure linearly increasing from 0 to 120 mmHg in 200 ms (corresponding to the systolic peak) to the ventricular side of the valve, for all analyzed cases. This approach significantly reduced the overall computational cost of the simulations, as well. Figure 3-10 describe quantitatively and qualitatively the difference noticed with the comparison between steady and pulsatile condition. The panel a, and b show qualitatively the shape of the valve from the top and axis view, respectively. No significantly differences can be noticed in term of systolic peak configuration. The panel c, shows, from a top-view, the stress distribution along leaflets. Some difference can be noticed on the contour color distribution in particular in the area around P1/P3 - C scallops. However, such a difference regards the stress distribution, but

not its magnitude. In the panel c the pressure load is compared with the simulated stress evaluated on P2 segments of the posterior leaflet for both the pressure conditions (red line = steady condition; light blue line = pulsatile condition). In terms of percentage, the difference between the two load conditions differs for less than 10 % at the systolic peak, as highlighted by the green circles in the plot.

3.5.4 Dynamic condition of the sutures tensioning

In all simulations, the tensioning was performed by imposing at the proximal nodes of the artificial sutures an outward displacement along the longitudinal direction. Such displacement promotes the reduction of the prolapsed portion of the posterior leaflet, since its margin moves towards the anterior one, as long as the repaired configuration is achieved (see Figure 3-11, panels a, and b).

In the first stage of the analysis, we simulated the clinical phase where the external sutures remain outside the ventricle before the tensioning stage. This stage is simulated by maintaining the four sutures no-tensioned until the achieving of the maximum pressure load so that the valve reached the idealized prolapse condition (see Figure 3-11). In the second stage of the analysis, two different strategies for restoring the valve coaptation were pursued. In the first one, indicated as all together strategy (AT) the four chords were tensioned contemporarily, by applying the displacement required to restore leaflets coaptation (Figure 3-11). In the second strategy, indicated as one by one strategy (1by1), the chords were tensioned one at a time by applying the same displacement as the AT case. In all simulations, the tensioning was performed by imposing at the proximal nodes of the artificial sutures an outward displacement along the longitudinal direction (see Figure 3-11, panel c). Such displacement promotes the reduction of the prolapsed portion of the posterior leaflet, since its margin moves towards the anterior one until the repaired configuration is again achieved. The prescribed displacement to obtain the proper coaptation length, for the simulated entry site, was estimated equal to 11 mm. This value was defined after some preliminary analysis by tuning the chords displacement until the maximum coaptation length between the anterior and posterior free margin was measured at the anterior-posterior axis (see Figure 3-2).

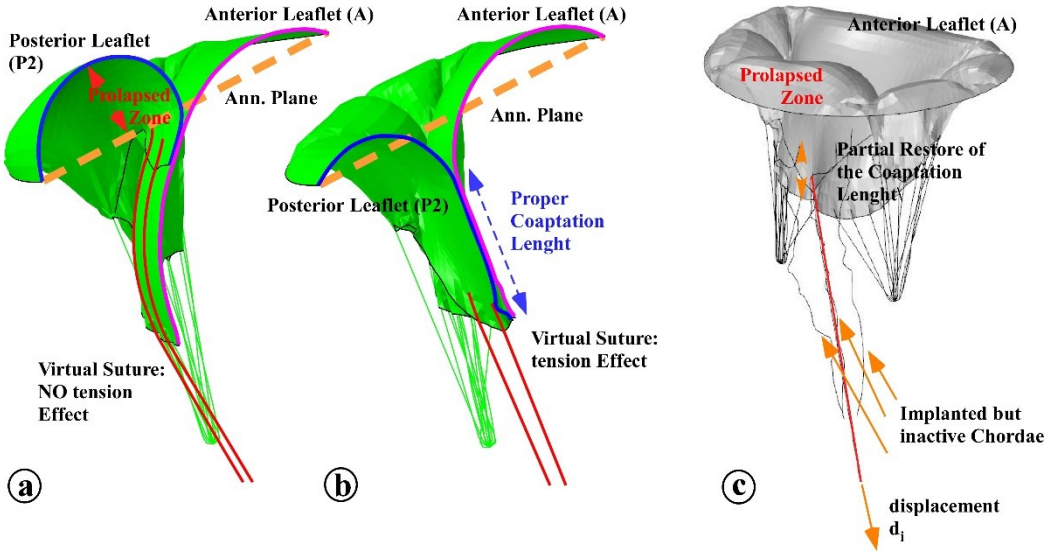

Figure 3-11 *Simulation of the artificial repair: dynamic BC for the simulation of the tensioning: a) Axis-view of the implanted but inactive sutures with the simulation of the P2 central prolapse; b) Final restoration of the valve with the complete recover of the proper coaptation length; c) schematic representation of the dynamic pull simulated for the 1by1 sequence.*

3.6 Results and Discussion

The healthy configuration of the generalized MV model produced a leaflets coaptation length along the axis of symmetry of about 8 mm (see Figure 3-9), corresponding to a total contact area, $A_{c,H}$, between the anterior and posterior leaflet of about 270 mm^2. The contact area, A_c, restored during neochords tensioning procedures, normalized with Ac,H is reported in Figure 3-12.

Figure 3-13 shows the contour map of the stress field computed on the treated leaflet P2 for all analyzed configurations. A scale from 0 to 0.5 MPa was chosen to better visualize the areas of stress concentration. The maximum stress reached at any point of P2 was determined, and its evolution upon a time is summarized in Figure 3-14, irrespective of the position on the scallop where it was recorded.

Finally, since neochord tensioning was simulated by imposing a displacement, the corresponding force along the sutures was calculated. Figure 3-15 describes the variation of the force in time for each of the four implanted neochords, for both AT (panel a) and 1by1 strategies (panels b-d).

MV prolapse repair has the function of restoring proper leaflet coaptation. Hence, the computed contact area at the systolic peak, A_c, normalized over the contact area estimated in healthy conditions, provides an indication of the efficacy of the procedure, as shown in previous similar work by Rim et al, [4], and Sturla et al, [15]. The results reported in Figure 3-12 suggest that MV functionality restoration is reached for both AT and 1by1 strategies.

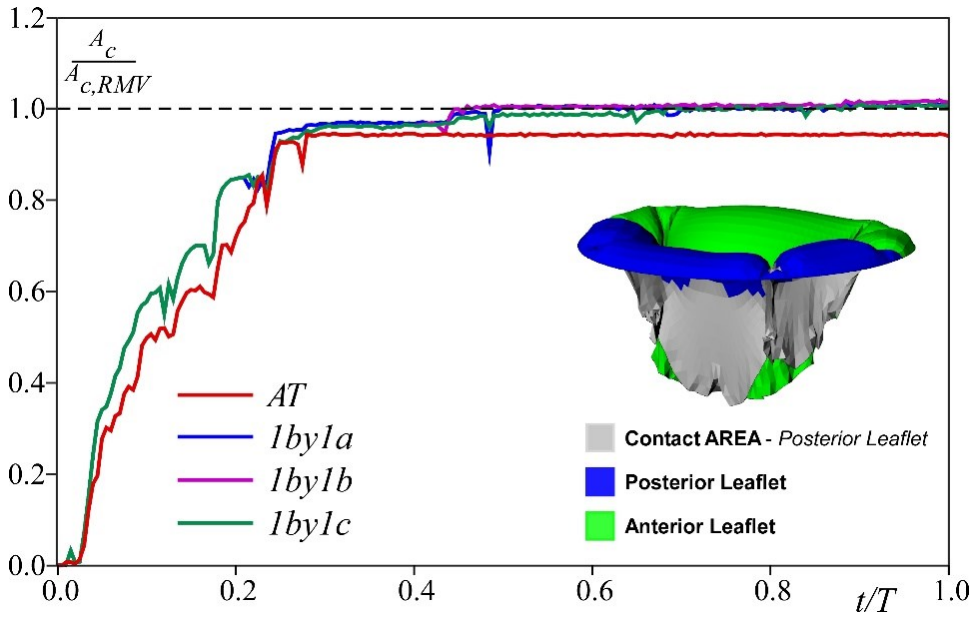

Figure 3-12 *Overall contact area on the Posterior leaflet during chord tensioning normalized with the contact area of the healthy configuration Ac,H. Red line represents AT strategy, blue, magenta and green lines represent 1by1 strategies following sequence a), b) and c) of Figure 3-1, respectively.*

For the AT strategy, the achieved coaptation area is about 95 % of the healthy value $A_{c,H}$; whilst with the 1by1 strategy $A_{c,H}$ is matched or even slightly exceeded. It is also worth noting that, in the case of the 1by1 scheme, the first neochord tensioning already results into a coaptation area equal to the 90 % of $A_{c,H}$, suggesting that MV restoration could be achieved by means of just one suture, for the present type of prolapse. However, as discussed below, the use of multiple chords allows to better diffuse stresses over a larger leaflet region, similarly to the physiological case, and distribute the load between the different chords.

The stress distribution on the valvular apparatus reported in Figure 3-13 shows that, for the prolapsed configuration, portion P2 experiences stress levels similar to the healthy case, while high-stress regions appear located at the adjacent portions of P1 and P3 scallops, close to the position of native chords rupture, in agreement with the literature [7]. The stress pattern after the procedure is similar to the healthy case, for both AT and 1by1 tensioning. However, in 1by1 simulations significantly higher stress levels are obtained at different stages of the procedure.

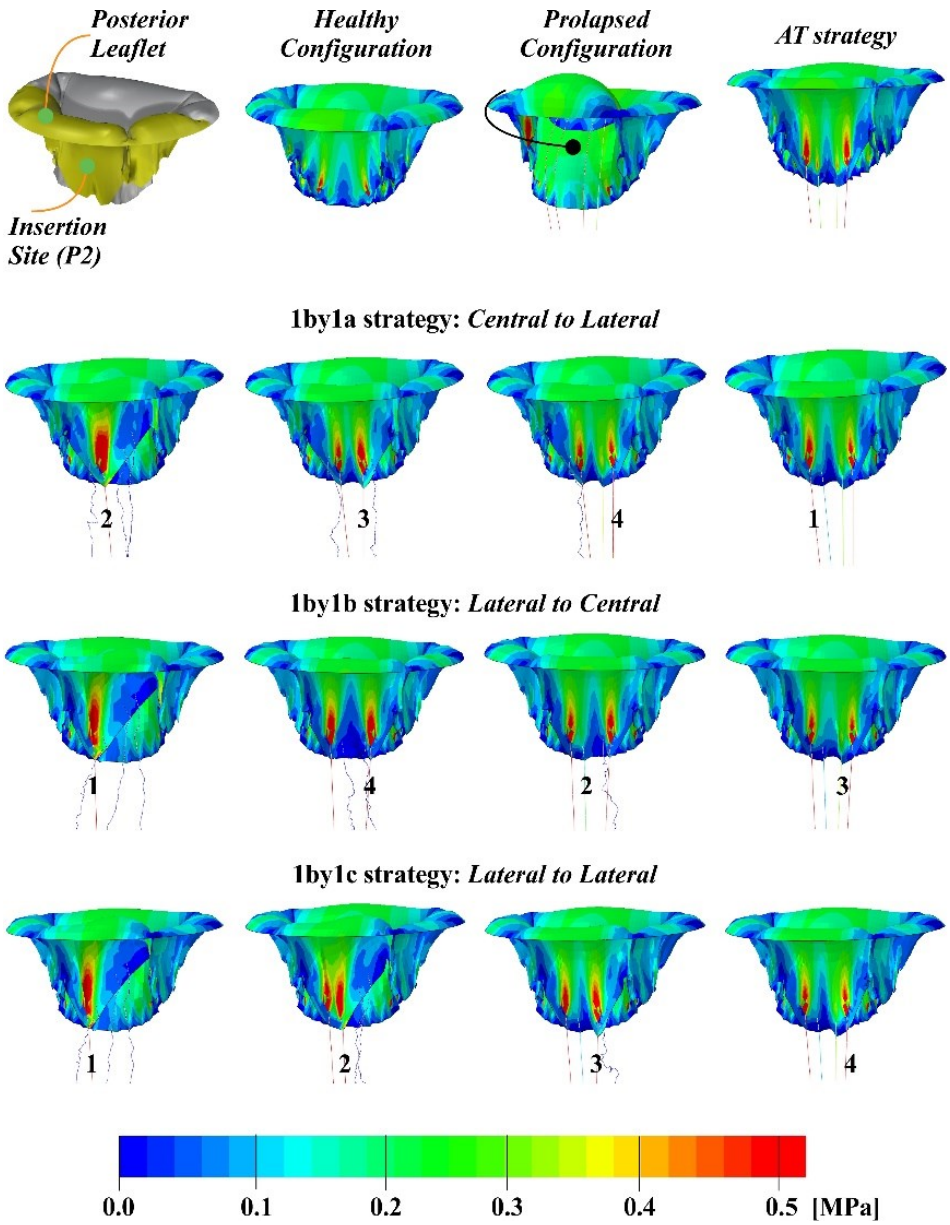

Figure 3-13 *MV stress patterns at systolic peak. Leaflet stress in healthy configuration, prolapsed configuration with inactive neochords, AT strategy configuration, and 1by1 strategy at different steps of pulling. The stress field in 1by1 cases is reported after the complete load of the neochord labeled by the irrespective number.*

In particular, the first chord pulling causes high stress in one region around the chord insertion site. This effect is clearly mitigated after the second chord pulling, with high stress redistributed in two smaller regions; then, tensioning of the third and fourth chord reduces only slightly the amplitude of high-stress regions and transfers the stress concentration in proximity to the external chords insertion. The results are partially supported by the works of Rim et al, [4], and Sturla et al, [15], which focus on the MV restoration by chords replacement considering neochordoplasty, i.e. a different surgical technique, carried out through the classical open-chest surgery. In particular, they tested a virtual repair, at peak systole, of prolapsed MV and its mitigation by implanting different numbers of chordae.

The results, both in terms of stress reduction and distribution, on the posterior leaflet are consistent with the results of the present analysis. In fact, the same behavior in term of maximum stress concentration at the external sutures is observed at the end of the procedure, showing analogous maximum stress level (difference about 10%) [4].

In Figure 3-14, the analysis of the maximum stress on the valve, σ_{max}, indicates that the 1by1 strategy gives very similar results to the healthy case, at the end of the procedure (σ_{max} around 1.5 MPa). On the contrary, AT procedure results in σ_{max} of about 1.9 MPa, i.e. 27% larger than the healthy case. Though higher values are reached during the 1by1 procedure, when the first chord is pulled, with a σ_{max} of about 2.5 MPa for 1by1a, the other tensioning sequences lead to levels of stress during the implant which is not substantially larger than for the AT procedure (2.1 MPa for 1by1b and 1by1c).

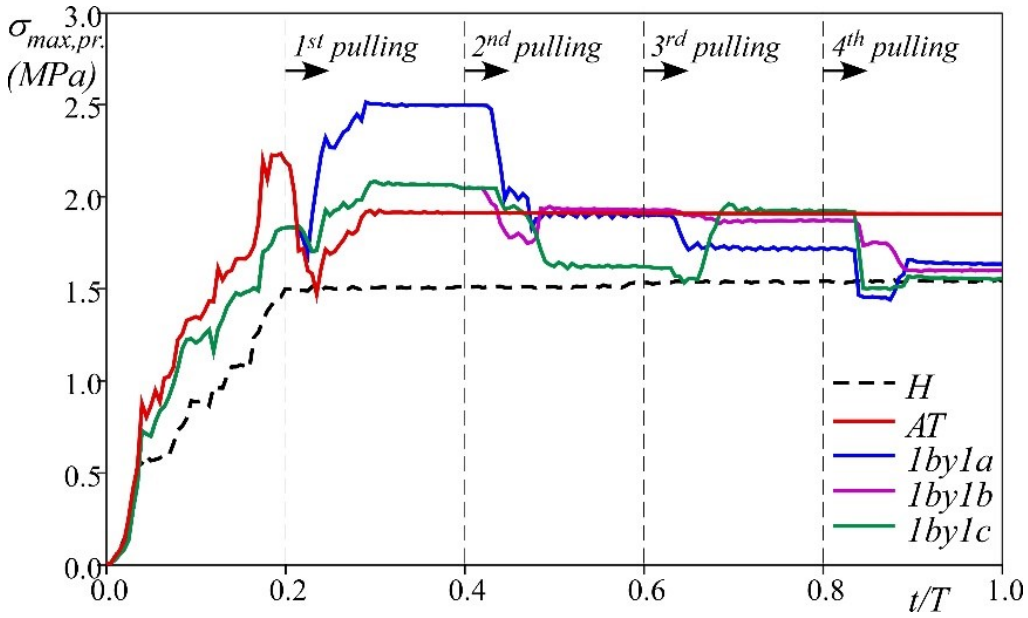

Figure 3-14 *Maximum principal stress calculated on the P2 scallop during simulations. The black dotted line represents the stress calculated for the Healthy configuration (H). The red line represents the AT strategy. The blue, magenta and green lines represent 1by1 strategies following sequence a), b) and c) of Figure 3-1, respectively.*

The stress distribution on the leaflets is related to the tensile force measured in the sutures (see Figure 3-15). Neochords pulled according to the AT procedure are subjected to a symmetrical force distribution, with a difference of about 30% between the force acting on the central and lateral insertions (0.2 N and 0.3 N, respectively, see Figure 3-15 a). 1by1 simulations show that the tensioning order affects the measured force. Specifically, tensioning a chord reduces the force applied to the chords previously pulled, and the reduction strongly depends upon the maneuver order and chords position. For instance, in

the 1by1a case (Figure 3-15 b) the force on the neochord pulled first (neochord 2) diminishes as soon as neochord 3 is pulled (F reduction around 50%), with a further reduction when neochord 1 is pulled (F reduction around 40%); i.e., the force on a chord reduces as soon as nearby chords become active. Results also show that no symmetry can be recognized in the final force distribution with respect to either neochord position or tensioning order. Moreover, the force is found to vary in the range 0.3-0.4N for the external chords and in the range 0.1-0.2N for the central one, showing that the maximum force difference between lateral and central artificial elements can be as large as 80%. The latter finding suggests that a central neochord can possibly result approximately unloaded at the end of neochords implantation, as reported by surgical clinical practice.

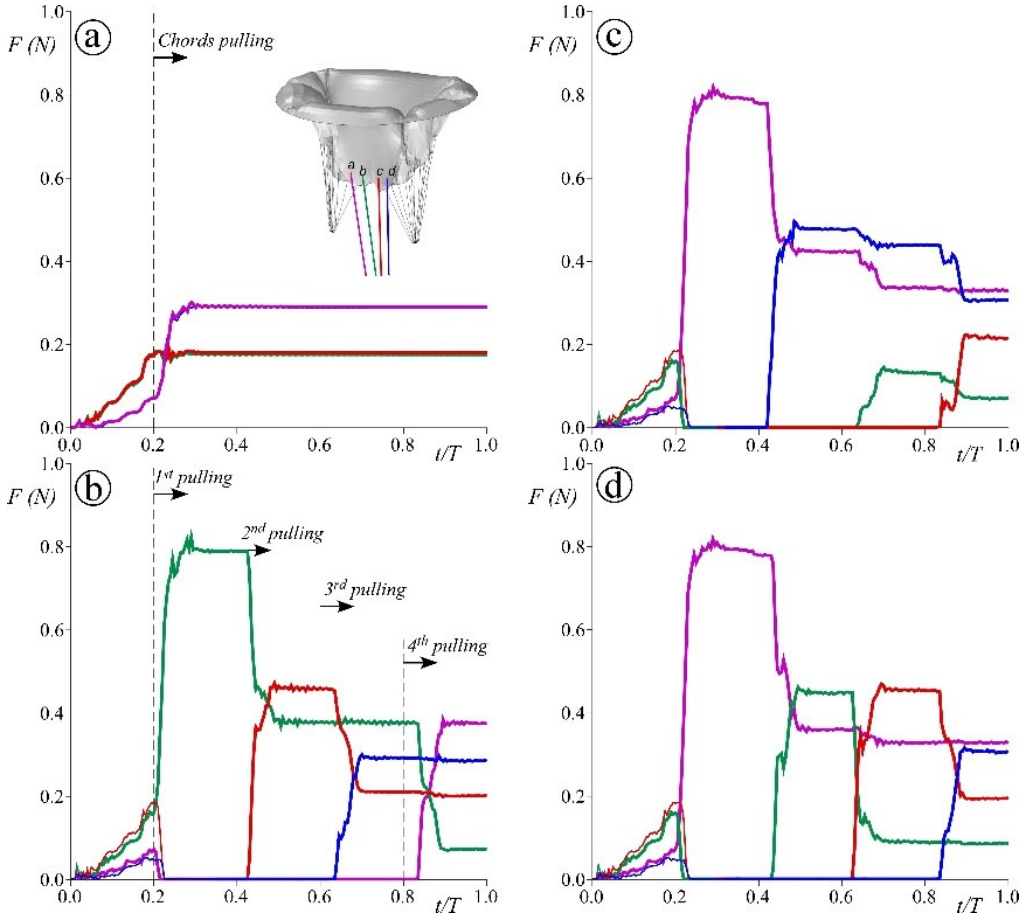

Figure 3-15 *Force applied by neochords during the implant in a) AT strategy, b) 1by1a (central to lateral sequence), c) 1by1b (lateral to central sequence), and d) 1by1c (lateral to lateral sequence).*

In all cases, the force on one neochord is well below the failure force of the suture, which is about 16 N, according to the GORE-TEX® SUTURE ePTFE manual. Finally, values of end procedure force applied to each neochord (see Table 3-3) also show that the overall force on the group does not significantly vary between the four simulated strategies of

pulling, further reinforcing the idea that differences in force repartition is due to the pulling sequence. In summary, AT procedure guarantees an almost symmetric distribution of tensioning force on the neochords, but does not fully restore the healthy contact area and produces higher stress levels on the valve. 1by1 strategies allow to optimize the coaptation area and post-procedural leaflet' stress, regardless the tensioning order but may result in almost inactive chords if attention is not given to this aspect. Among the 1by1 strategies, the central to lateral tensioning sequence proved to be the least appropriate, as it results in very high levels of procedural stresses acting on the leaflets. This can be avoided by adopting a lateral to central or lateral to lateral approach, which cause procedural stresses similar to the AT procedure, with substantially lower post-procedural stresses and full restoration of the coaptation area.

Table 3-3 *Forces calculated on the neochords after the implantation of the four cases analyzed. Forces are expressed in N.*

	neochord				**Tot.**
	a	**b**	**c**	**d**	
AT	0.29	0.18	0.18	0.29	0.94
1by1a	0.37	0.07	0.20	0.28	0.93
1by1b	0.33	0.07	0.21	0.31	0.92
1by1c	0.33	0.09	0.20	0.31	0.92

3.7 Conclusion

The present investigation compares the two most common tensioning procedures adopted in the transapical neochords implantation for mitral valve prolapse repair, i.e. 'all together' and 'one by one' pulling approach. The study was performed on a generalized MV morphology, with prolapsed P2 scallop. Although idealized geometries and simplified constitutive behaviors were assumed, the study captures some of the clinical effects observed by surgeons, e.g. the unloading of previously pulled neochords.

The close similarity between healthy and repaired configuration obtained for all investigated strategies confirms the reliability and efficacy of the preferred surgical choice of four chords to treat the prolapse here considered.

Differences found in the results concerning coaptation area, stress distribution, and force on the neochords for AT and 1by1 repair suggest that the 1by1 lateral to central and lateral to lateral approaches are the most suitable solutions to reach maximum coaptation and maintaining operative leaflets stresses close to those experienced in healthy conditions, without increasing substantially the procedural stresses respect to the AT strategy.

The present study is limited to the P2 central prolapse, i.e. the most common MV prolapse. A different stress force distribution may be expected for the lateral (P1-P2 or P2-P3) and the anterior (A) prolapse. In particular, in the former, due to its asymmetry, the tensioning of the suture is more likely to depend on the pulling strategy.

The use of both more realistic geometric configuration and more physiologic boundary condition can further improve the results and highlight additional aspects of the NeoChord implant. It can be foreseen that, lastly, application of the presented approach to patient-specific anatomies may provide a useful tool for procedural planning, improving the efficacy of the treatment.

Indeed, though this first study was based on a generalized symmetrical model, the robustness and reduced computational cost of the presented methodological approach makes it is suitable to be adopted for the clinical planning of the treatment in patient-specific cases. It would help highlight potential critical issues of the different tensioning maneuvers connected with the individual characteristics of the MV prolapse under treatment, making it possible to design an optimum procedure.

3.8 Appendix A (p1-p2 prolapse simulation)

In the present appendix, a different prolapse position with the same mitral valve geometry was investigated. This analysis was performed in order to investigate the numerical restore feasibility for a different prolapse position, technically more challenging of the central one investigated in this chapter. The MV incompetence was then simulated by detaching five lateral chords around the P1-P2 segment, leading to a non-symmetrical prolapse (see panels a-b of Figure 3-16).

Both tensioning protocols and the number of artificial sutures was able to restore a proper contact area and physiological closure like the heathy reference case. However, what is worth noting from this simulation is represented in the panel d and e of Figure 3-16. Despite the simplifications assumed for both leaflets geometry and native chordae distribution, has been highlighted the probable interference between the artificial sutures and the native chordae if the sutures are implanted following a non-symmetric trajectory due to the non-symmetric area interested by the prolapse. This evidence was confirmed and reported in some clinical papers, at the beginning of the NeoChord procedure experience, where clinicians describe the native chordae rupture as the consequence of a criss-crossing between native chordae and artificial ones, leading to scratching, deterioration and finally rupture of the native sub-valvular mitral apparatus, [1], [7]. Further simulations and

quantitative analyses of the problem must be done to better understand the un-physiological contact between different structures. Further improvement could be obtained with a study, according to clinical feasibility, of a different entry site for the restore of a non-symmetric posterior prolapse.

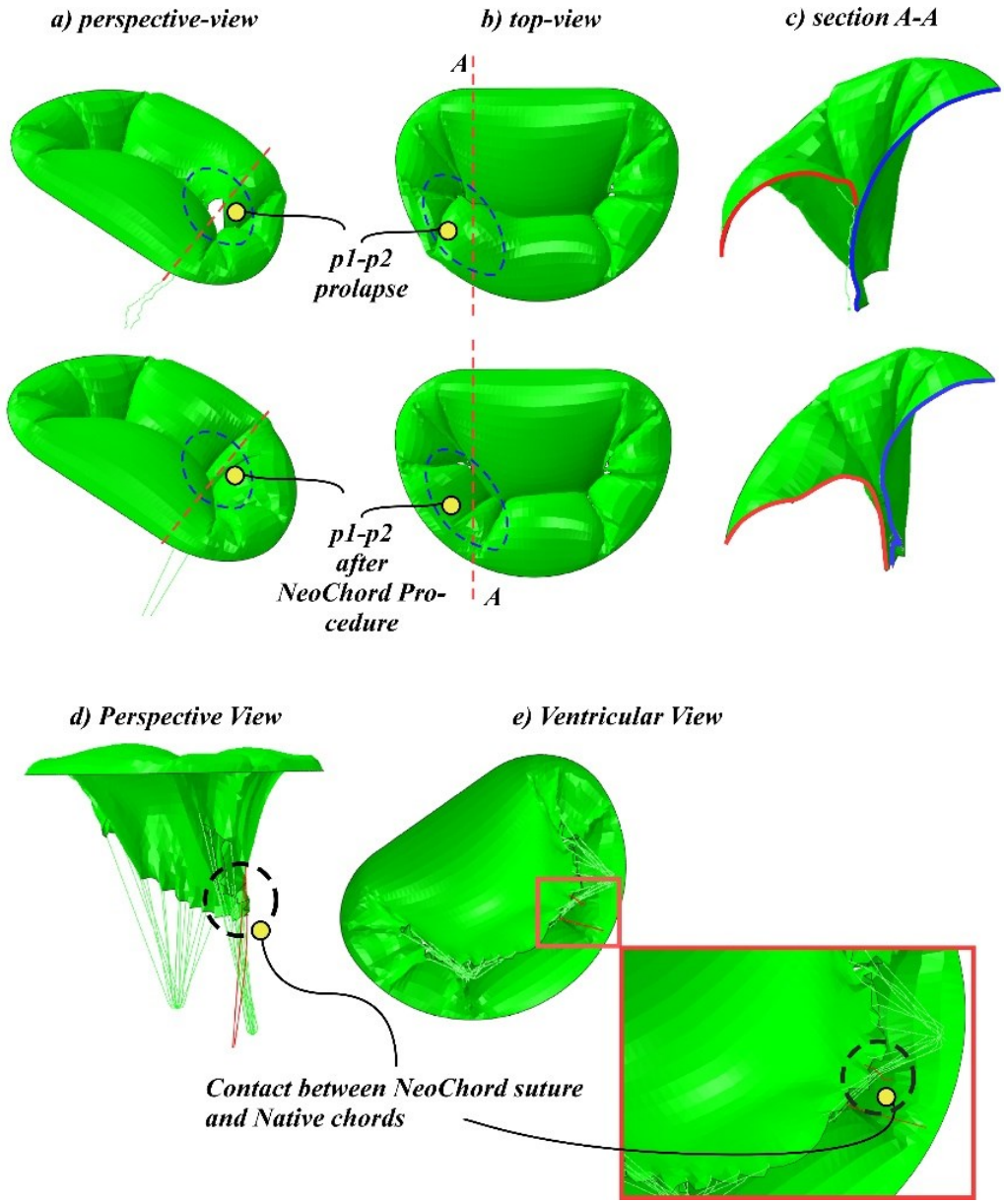

Figure 3-16 *Simulation of a non-symmetrical prolapse (P1-P2 segment of the posterior leaflet). The panels a, b, and c shows the effectiveness of the restore with different points of view; the panels d, and e, describe the possible interaction between artificial sutures and native chordae due to the non-symmetric trajectories of the sutures, as well as, due to the non-symmetric position of the posterior prolapse.*

3.9 Reference

[1] G. Biglino, C. Capelli, J. Bruse, G. M. Bosi, A. M. Taylor, and S. Schievano, "Computational modelling for congenital heart disease: How far are we from clinical translation?," *Heart*, vol. 103, no. 2, pp. 98–103, 2017.

[2] E. Votta *et al.*, "Toward patient-specific simulations of cardiac valves: State-of-the-art and future directions," *J. Biomech.*, vol. 46, no. 2, pp. 217–228, 2013.

[3] A. Choi, D. D. Mcpherson, and H. Kim, "Computational virtual evaluation of the effect of annuloplasty ring shape," *Int. j. numer. method. biomed. eng.*, vol. 02831, no. September, pp. 1–11, 2016.

[4] A. Avanzini, G. Donzella, and L. Libretti, "Functional and structural effects of percutaneous edge-to-edge double-orifice repair under cardiac cycle in comparison with suture repair," *Proc. Inst. Mech. Eng. Part H J. Eng. Med.*, vol. 225, no. 10, pp. 959–971, 2011.

[5] F. Domenichini and G. Pedrizzetti, "Hemodynamic forces in a model left ventricle," *Phys. Rev. Fluids*, vol. 1, no. 8, pp. 1–20, 2016.

[6] M. S. Reimink, K. S. Kunzelman, E. D. Verrier, and R. P. Cochran, "The Effect of Anterior Chordal Replacement on Mitral Valve Function and Stresses: A Finite Element Study.," *Asaio J.*, vol. 41, no. 3, pp. M754--M762, 1995.

[7] Y. Rim, S. T. Laing, D. D. McPherson, and H. Kim, "Mitral Valve Repair Using ePTFE Sutures for Ruptured Mitral Chordae Tendineae : A Computational Simulation Study," *Ann. Biomed. Eng.*, vol. 42, no. 1, pp. 139–148, 2014.

[8] F. Sturla *et al.*, "Biomechanical drawbacks of different techniques of mitral neochordal implantation: When an apparently optimal repair can fail," *J. Thorac. Cardiovasc. Surg.*, vol. 150, no. 5, pp. 1303–1312, 2015.

[9] A. Colli *et al.*, "Acute safety and efficacy of the NeoChord procedure," *Interact. Cardiovasc. Thorac. Surg.*, vol. 20, no. 5, pp. 575–581, 2015.

[10] K. D. Lau, V. Diaz, P. Scambler, and G. Burriesci, "Medical Engineering & Physics Mitral valve dynamics in structural and fluid – structure interaction models," *Med. Eng. Phys.*, vol. 32, no. 9, pp. 1057–1064, 2010.

[11] K. S. Kunzelman, D. R. Einstein, and R. P. Cochran, "Fluid-structure interaction models of the mitral valve: Function in normal and pathological states," *Philos. Trans. R. Soc. B Biol. Sci.*, vol. 362, no. 1484, pp. 1393–1406, 2007.

[12] A. Colli *et al.*, "Prognostic impact of leaflet-to-annulus index in patients treated with transapical off-pump echo-guided mitral valve repair with NeoChord implantation," *Int. J. Cardiol.*, vol. 257, no. November 2015, pp. 235–237, 2018.

[13] A. Colli *et al.*, "Transapical off-pump mitral valve repair with Neochord Implantation (TOP-MINI): step-by-step guide," *Ann. Cardiothorac. Surg.*, vol. 4, no. 3, p. 295, 2015.

[14] A. Colli *et al.*, "CT for the Transapical Off-Pump Mitral Valve Repair With Neochord Implantation Procedure," *JACC Cardiovasc. Imaging*, vol. 10, no. 11, pp. 1397–1400, 2017.

[15] A. Colli, R. Bellu, D. Pittarello, and G. Gerosa, "Transapical off-pump Neochord implantation on bileaflet prolapse to treat severe mitral regurgitation," *Interact. Cardiovasc. Thorac. Surg.*, p. ivv192, 2015.

[16] A. Colli *et al.*, "Transapical off-pump mitral valve repair with Neochord implantation: Early clinical results," *Int. J. Cardiol.*, vol. 204, pp. 23–28, 2016.

[17] A. Colli *et al.*, "Patient-Specific Ventricular Access Site Selection for the NeoChord Mitral Valve Repair Procedure," *Ann. Thorac. Surg.*, vol. 104, no. 2, pp. e199–e202, 2017.

[18] K. Kunzelman, R. P Cochran, S. S Murphree, W. S Ring, E. Verrier, and R. Eberhart, *Differential collagen distribution in the mitral valve and its influence on biomechanical behaviour*, vol. 2. 1993.

[19] R. P. COCHRAN, K. S. KUNZELMAN, C. J. CHUONG, M. S. SACKS, and R. C. EBERHART, "Nondestructive Analysis of Mitral Valve Collagen Fiber Orientation," *ASAIO J.*, vol. 37, no. 3, 1991.

[20] K. May-Newman and F. C. Yin, "Biaxial mechanical behavior of excised porcine mitral valve leaflets," *Am. J. Physiol. Circ. Physiol.*, vol. 269, no. 4, pp. H1319--H1327, 1995.

[21] K. Kunzelman, M. S. Reimink, E. D. Verrier, R. P. Cochran, and R. W. M. Frater, "Replacement of Mitral Valve Posterior Chordae Tendineae with Expanded Polytetrafluoroethylene Suture: A Finite Element Study," *J. Card. Surg.*, vol. 11, no. 2, pp. 136–145, 1996.

[22] H. Muresian, "The clinical anatomy of the mitral valve," *Clinical Anatomy*, vol. 22, no. 1. pp. 85–98, 2009.

4 Mitral Valve Model and Simulations: Access Site Selection for NeoChord Procedure

4.1 Introduction

In the last years, the transapical off-pump Mitral Valve (MV) repair with artificial chords implantation has emerged as a promising intervention to restore MV function in degenerative disease (see Chapter 2). At present, the procedure is mainly performed using one device (*The NeoChord DS1000 system*), which implants the neochord at the leaflet free margin through a postero-lateral ventricular attachment. Recently, an alternative device, The Harpoon Mitral Valve Repair System *(H-MVRS)*, has been proposed to treat the MV disease implanting the artificial chords more deeply into the body of the leaflet through an anterior ventricular attachment (see Figure 4-1). The aim of the present study is to quantify by numerical simulations pros and cons of the two procedures for different prolapse types according to the classification proposed by Adams et al., [1], namely the Fibroelastic Deficiency *(FED),* the *Forma Frusta (FF),* and the *Barlow (B)*.

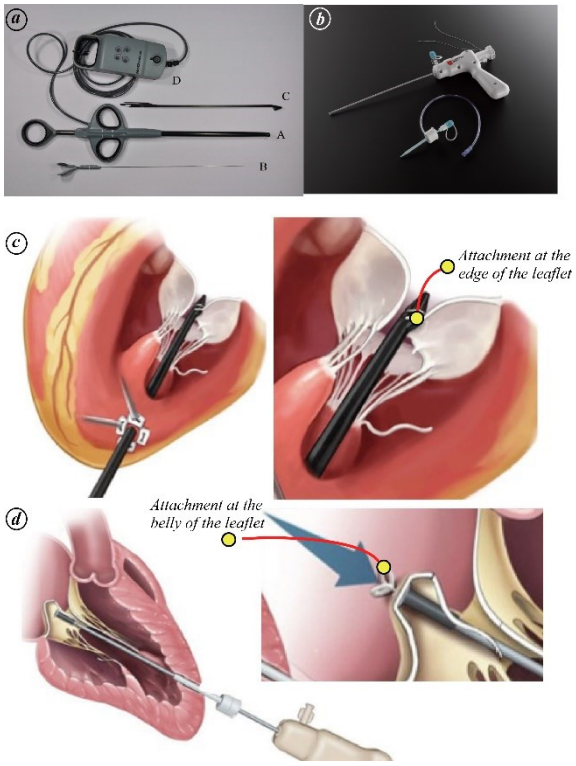

Figure 4-1 *Devices comparison: a) the NeoChord DS1000 system, b) the Harpoon Mitral Valve Repair System, c) and d) technical attachment on the leaflet for both devices. Figure from Lancellotti et al., [2].*

In this section is presented a new approach for the realization of patient-specific MV domains, which are employed to implement more realistic simulations of the neochord

procedure. The present study describes all the possible scenarios of the MV prolapse disease and the related numerical analysis are carried out aiming at investigating the performance of the two devices. A possible optimization of the implants procedures is investigated for both the *apparati*, as well. In particular, different trajectories of artificial sutures are investigated in terms of the closure of the valve (namely, the contact area between leaflets), the tensioning forces and the additional stress on the leaflet due to the implant of the sutures.

4.2 The Access Sites Investigated

Numerical simulations were carried out on three types of posterior prolapses, whose classification varies according to the grade of degenerative mitral valve disease proposed by Adams, [1].

MV anatomies were extracted based on echocardiographic 3D datasets of 170 patients treated with both procedures at the Department of Cardiology, Thoracic and Vascular Sciences of the University of Padua, [3], [4].

All the anatomical characteristics and detailed realization process are described in the remainder of the chapter.

For each prolapse type (*FED*, *FF*, and *B*), we analyzed the following four scenarios:

- **NeoChord device (The NeoChord DS1000 system)**

a1) standard procedure: the insertion point of the suture is about 4 mm far from the leaflet free margin with the postero-lateral ventricular access site (reference case – and the reference angle of α=0°) see Figure 4-2;

a2) procedure modification: the insertion point of the suture is about 4 mm far from the leaflet free margin with the anterior ventricular access site (working angle of 40°).

- **Harpoon device (The Harpoon Mitral Valve Repair System (H-MVRS))**

b1) procedure modification: the insertion point is about 8 mm far from the margin (leaflet belly) with the postero-lateral ventricular access site (angle of 0°).

b2), standard procedure: the insertion point is about 8 mm far from the margin (leaflets belly) with the anterior ventricular access site (working angle of 40°).

Figure 4-2 shows schematically the trajectories and the working angles of the artificial sutures moving the access site from the posterior to the anterior position.

The reference trajectory ($\alpha=0°$) is defined along the posterior access site (blue line). The anterior working angle is set at $\alpha=40°$ (red line), according to the technical procedure indicates for the clinical operative phase.

Here, the panel *a,* and *b* show a schematic 3D heart reconstruction and a volume render cardiac tomography reconstruction, respectively, highlighting the two entry site associated with different trajectories of the artificial sutures.

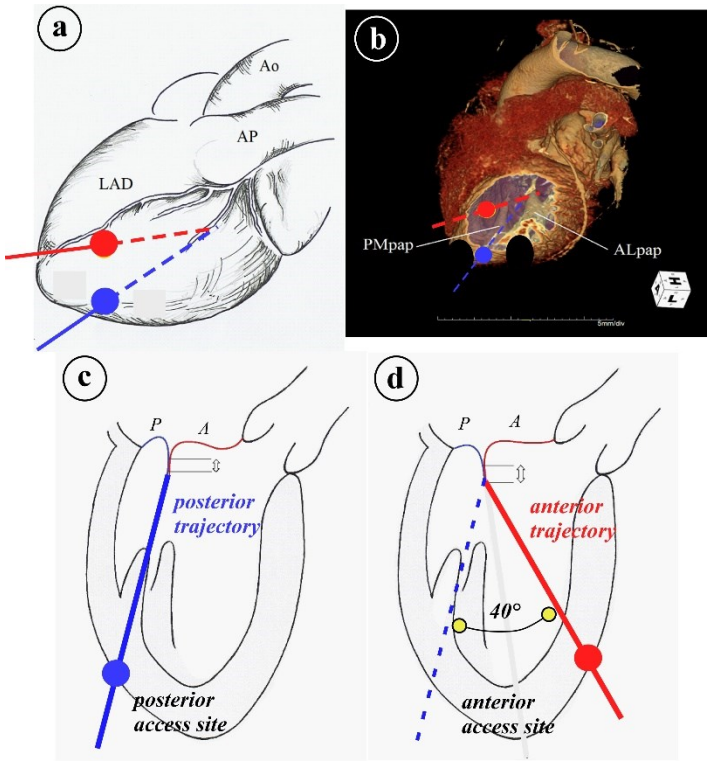

Figure 4-2 *Access site identification: panel a), and b): endocardial position of each entry site, indicated with PMpap (Post-medial papillary muscle) and ALpap (Antero-Lateral papillary muscle) the pupillary muscles; c), and d): schematic long-axis ventricular view of the two ventricular access site location and they respective artificial suture trajectory. Blu line indicates reference access site and working angle (α=0°). Red line indicates more anterior working angle set to α=40° a part from the reference case. Figure from Colli et al.,*[5].

The solid circles identify the endocardial position of each entry site. In particular, the panel b shows the position related to the papillary muscles (PMs). The blue circle represents the proximally the midpoint between the two PMs and is defined as posterior access site, while the red circle is placed more anterior and superior. In this case, the suture trajectory is guided across the left ventricle outflow tract.

The panels *c*, and *d* shows a schematic long-axis ventricular view of the standard NeoChord and Harpoon trajectory implantation, respectively.

4.3 Mitral Valve Model

4.3.1 Geometry

An imaging post-processing was applied to derive the three different MV patient-specific models in according to the criteria proposed by Adams, [1], to recognize the common typologies of the MV prolapse, i.e. the Fibroelastic Deficiency *FED,* the Forma Frusta*,* and the Barlow. The echo images are provided from three patients belonging to a cohort of 160 units affecting by mitral regurgitation (MR) at the Padua Cardiac Surgery Unit, and they are acquired during both pre- and intra-operative NeoChord procedure phases.

The approach adopted has been recently developed by our collaborators at University College London, UK, (S. Schievano and B.Biffi). The model is based on the analysis of clinical imaging (3D echo and CT-scan) and is able to automatically segment the MV, and extract several morphological parameters of interest necessary for the numerical dynamic analysis. Specifically, the algorithm computes the following output parameters: antero-posterior diameter (APd), intecommissural distance (LLd), anterior (AMLl) and posterior (PMLl) mitral leaflet lengths, leaflets surface (MLs), local and average leaflets thickness (MLt), annulus perimeter (MAp), and annulus surface (MAs).

In particular all the 3D-echo images are processed to obtain patient specific leaflets geometry information at end-diastole configuration (See Figure 4-3).

The 3D echo images (end diastole), acquired intra-operatively before NeoChord implant, are segmented via an atlas-based method able to automatically annotate MV leaflets and annulus, [6]. The obtained segmentations is converted into a smooth triangular mesh representations.

The automated modeling approach defines accurately the annulus and leaflets free margin profile. Further details of the main leaflets segments are supplied by the scan of the images, as well. In particular, the informations about the position of the PMS are estimated by manually analyzing the 3D-echo images of the ventricle.

Unfortunately, the images do not allow to identify the chords structures and, accordingly, they are assumed *a posteriori* by tuning the trajectories of the chords in a preliminary analysis as follows.

First, a set of native chordae is defined according to the papillary muscles position and the leaflets free margin profile. A preliminary closing simulations are then performed in order to determine the number, the length, and the distribution of such native chordae. The prolapse position is finally reproduced by detaching or elongating a limited number of

chordae as long as we find a good agreement between the simulated and the reconstruct prolapse.

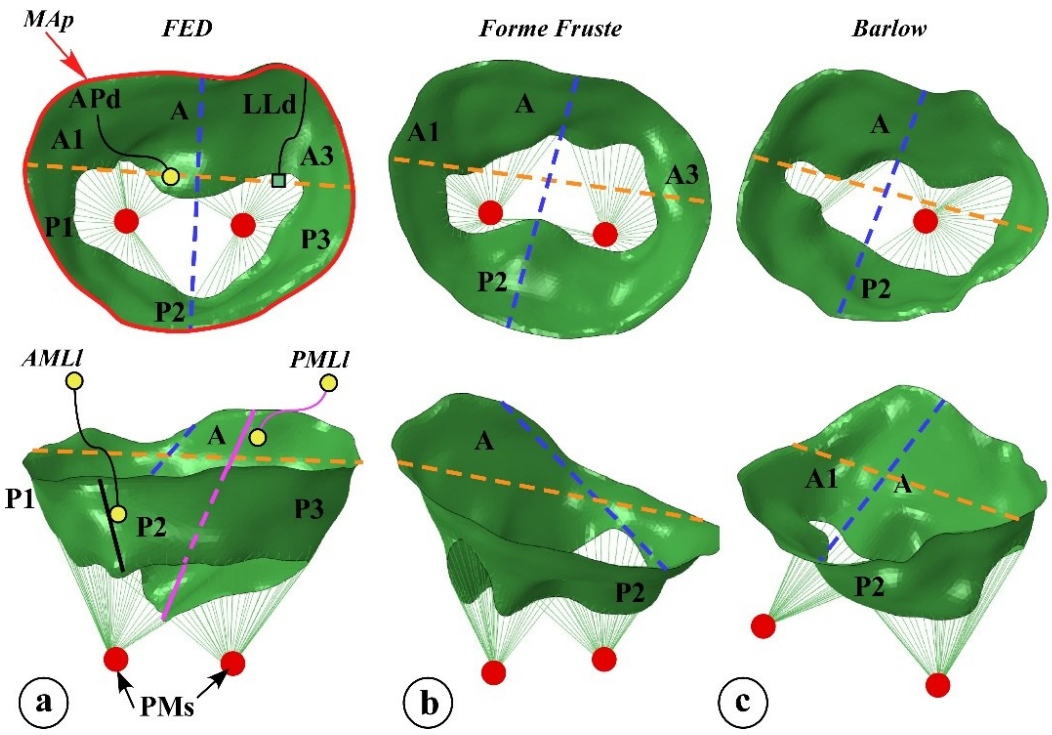

Figure 4-3 *MV geometry of the models at the end of diastole: From a) to c) Atrial (top-view) and lateral view (bottom) of FED, Forme Fruste and Barlow models, respectively. A indicates the anterior leaflet, A1 and A3 the commissural leaflet scallops, P1, P2 and P3 the posterior leaflet scallops, (APd), antero-posterior diameter (LLd) intecommissural distance , (AMLl) anterior and (PMLl) posterior mitral leaflet lengths, red line indicates MV annulus. CT the chordae thendinae, and PMs the papillary muscles*

Figure 4-3 shows the initial configuration of the MV leaflets and native chordae i.e. the end-diastolic phase for the three MVs investigated, highlighting all the main geometrical parameters. It is possible to identify all the leaflets segments (Anterior, Posterior and Commissural scallops, i.e., A1 and A3 segments) and to notice the PMs initial position.

All main parameters of MV geometries, e.g. the thickness, diastolic AP annulus, diastolic LL annulus, AML length, PML length, and cross-sectional area used for the leaflets and chordae in the various portions of the model, are summarized in Table 4-1.

The FED and FF patients present a P2 central prolapse with a flail width of 12 and 14 mm, respectively, whereas, the Barlow case presents a prolapse positioned around the P1-P2 segments, with a flail width of 16 mm.

Table 4-1 *main parameters of MV geometries: intecommissural distance (LLd), antero-posterior diameter (APd) anterior (AMLl) and posterior (PMLl) mitral leaflet lengths, leaflets surface (MLs), average leaflets thickness (MLt), annulus perimeter (MAp), and annulus surface (MAs).*

Prolapse Type	*LLd [mm]*	*APd [mm]*	*AMLl [mm]*	*PMLl [mm]*	*MLs [mm2]*	*MLt[mm]*	*MAp [mm]*	*MAs [mm2]*
FED	47.33	35.36	33.53	16.33	1956.09	1.31	143.87	1413.39
FF	46.87	41.17	35.54	25.20	2285.89	1.49	159.96	1672.64
BARLOW	46.32	42.01	35.40	25.81	2333.65	1.66	157.72	1614.18

4.3.2 Virtual Repaired Models

The MV function is restored by inserting three chords for the Barlow prolapse and four chords for the FED and the Forme Fruste prolapse, in agreement with the surgical clinical practice. In all cases, we restore the valve functionality firstly by setting all the sutures with the standard trajectories and secondly by modifying them one-by-one for each scenario. Figure 4-4 shows Top-View and Lateral-View of the virtual repairs with both working angles studied for each prolapse type. As explained previously, the virtual models differ for the position of the attached site of the sutures. (see Figure 4-5 for the detailed connection).

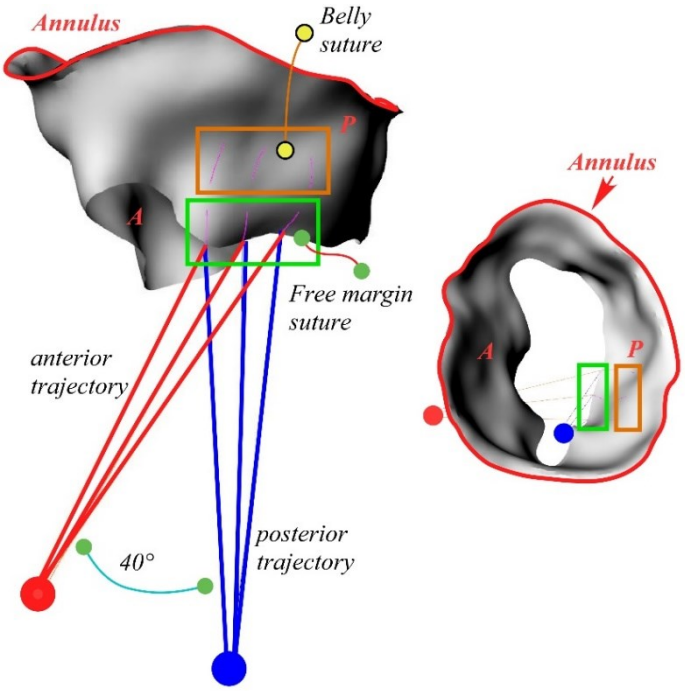

Figure 4-4 *Virtual repair model: The figure shows the virtual repair for the Barlow's disease with the application of three suture. The lateral (sx) and top view (dx) shows the working angles evaluated (blue line posterior access, red lines anterior access – 40°) and the different position around the diseased segment of the leaflet free margin suture (green) and the belly suture (orange)*

4.4 Mechanical Characterization

The same material model described in the previous chapter is used in the present simulations.

The leaflets are modeled as membranes, with the isotropic hyperelastic incompressible constitutive law based on a 5th order reduced polynomial strain energy potential formulation. The model coefficients are determined from mechanical tests performed on porcine mitral valves by May-Newman and Yin, [7], averaging data obtained along radial and circumferential direction (see Figure 3-4, Section 4). Finally, chords are modeled as linear elastic trusses, with Young modulus, $\boldsymbol{E}$, equal to 40 MPa, [8], [9];

The artificial sutures are represented by linear truss elements with a circular cross-section of 0.148 mm^2 (i.e. the sum of the cross-section of the two stands). The neochord's Young modulus is determined experimentally and set equal to 2.3 GPa.

For further detail see Chapter 3 - *Mitral Valve Model and Simulations: Tensioning Protocols for NeoChord Procedure*.

4.5 Numerical Simulations

The MV dynamics is simulated by means of the Finite Element Method provided by the commercial software for structural analysis ABAQUS 2016 (SIMULIA, Providence, RI).

As described in Chapter 3 the leaflets and both the native and artificial chords, are modeled by linear triangular membrane elements (2D elements – M3D3, 3 nodes triangular membrane) and truss (1D elements – T3D2, 2 nodes linear 3D truss), respectively.

As far as the connections among MV sub-elements concerning, we adopt the same method described in the Charter 3. The physiological intra-leaflets insertion of the native chords, which consists in the prolong of native chordae inside the leaflet (see Figure 4-5, panel a), is mimicked into the free margin, [10], by merging the leaflet and the chords nodes; i.e. merging the same nodes of the membrane and truss. The Neochord implant is simulated imposing the connection around the free margin of the diseased portion, whereas for the Harpoon implant the connection is made around the belly of the same prolapse segment (see Figure 4-5, panels b and c).

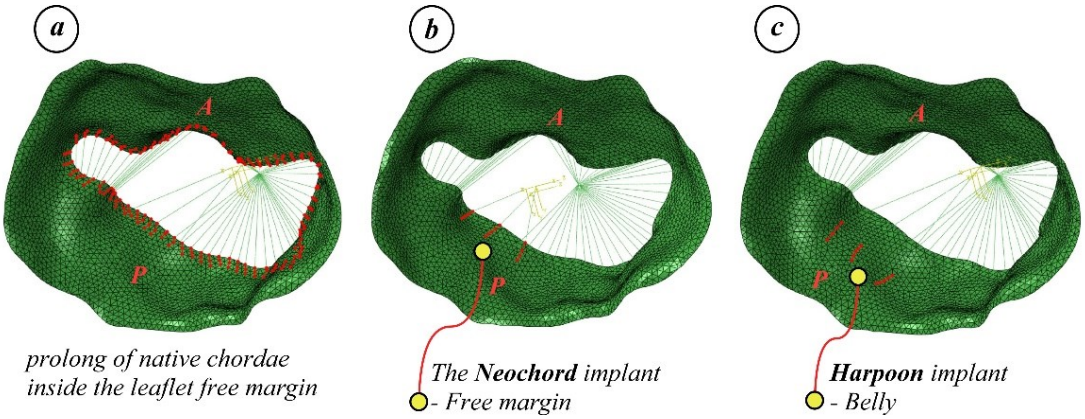

Figure 4-5 *Connections among both native chordae and artificial sutures with leaflet prolapse segment; a) intra-leaflet insertion of the native chordae; b) and c) NeoChord implant simulation (free margin) and Harpoon implant simulation (belly), respectively.*

The closed configuration of all the virtual repairs is achieved by applying a spatially uniform pressure on the ventricular side of the MV leaflets. As demonstrated previously, it has been chosen to describe the pressure condition with a pressure ramp that linearly increases from zero to the maximum pressure of 120 mmHg. After the systolic peak pressure, the load condition simulates a steady pressure, during which we artificially repair the valve, i.e. the simulation describes a series of systolic peak phases maintaining the closure position, without simulating the diastolic opening due to a pulsatile pressure load. In all cases, we maintain the annulus fixed during the closure, and we only allow the rotations of the leaflets elements about all axes (hinge condition). This choice has been preliminarily assessed by carrying out several simulations in order to quantify the effect due to the annulus motion on the tensioning. The results confirmed that the effect of the annulus dynamic does not affect the results in terms of the contact area, but a reduction both in terms of global tensioning forces was observed (about 10 %) and additional stresses on the leaflet at the attach zone of about 10 %. This effect is confirmed by the works of Votta-Stevanella and co-authors [11], [12], where they analyze with high accuracy the effect of both annulus dynamics and its shape in terms of MV dynamics and stresses response. On the other hands, to enhance the native chordae regulation and valve closure, the PMs displacements during the simulations are instead correctly reproduced by the clinical data provided by our collaborators at UCL. We prescribe to the PMs, represented as single points, two time-dependent 3D trajectories, whilst the native chordae are pinned at these points just allowing the rotation of the truss elements. In such way, the chordae are in-built with both the PMs and the leaflet free margin.

The tensioning occurs similarly to the previous analysis of tensioning protocols (Chapter 3). At the proximal nodes of the sutures, we prescribe an outward displacement along the

longitudinal direction of the initial trajectory of the suture itself. The dynamic displacement imposes to the sutures starts once the maximum pressure load is reached, thus simulating the pre-tensioning configuration of the implant, as well. During this phase, all the sutures are free to move following the leaflet dynamic.

The artificial chords are tensioned all together applying to each chord the same displacement in according to the AT tensioning approach. It is worth noting that the displacement that ensures the maximum coaptation area varies for each scenario being strictly dependent on the access site and the suture position into the leaflet. Accordingly, we fix the maximum displacement to 10 mm, i.e. a value large enough to include the repositioning that produces the best valve performance after the repair, and, during the simulated time, we linearly change the position of the chords (see Figure 4-6 a – linear displacement imposed as a dynamic condition). For each entry site, therefore we are able to identify the tensioning configuration that maximizes the coaptation length between anterior and posterior leaflets.

4.6 Results and Discussion

4.6.1 Extraction of the results and description of the simulation approach

All the numerical simulations performed permit to quantify all the main parameters able to evaluate the effectiveness of the repair and to easily compare the results for all the scenarios considered in the analysis.

In particular, the most important index for assessing the MV restoration are the contact area between leaflet at the closure and the corresponding coaptation length measured along the axis of symmetry of the MV model (see Figure 4-3).

This quantity has been chosen as a target point for all the simulations, i.e., the computed value that confirms the success of the MV restoration. When this quantity reaches the maximum value during the increase of the simulated pull, it is defined the optimal values of forces and displacement able to restore the prolapse, and the evaluation of the maximum additional stresses that affect the leaflet.

For instance, Figure 4-6 shows all the parameters considered during the simulation of the repair performed with the NeoChord technique, which is characterized by the point of attachment in correspondence of the leaflet free margin and the posterior entry site, i.e. the working angle is $\alpha=0°$.

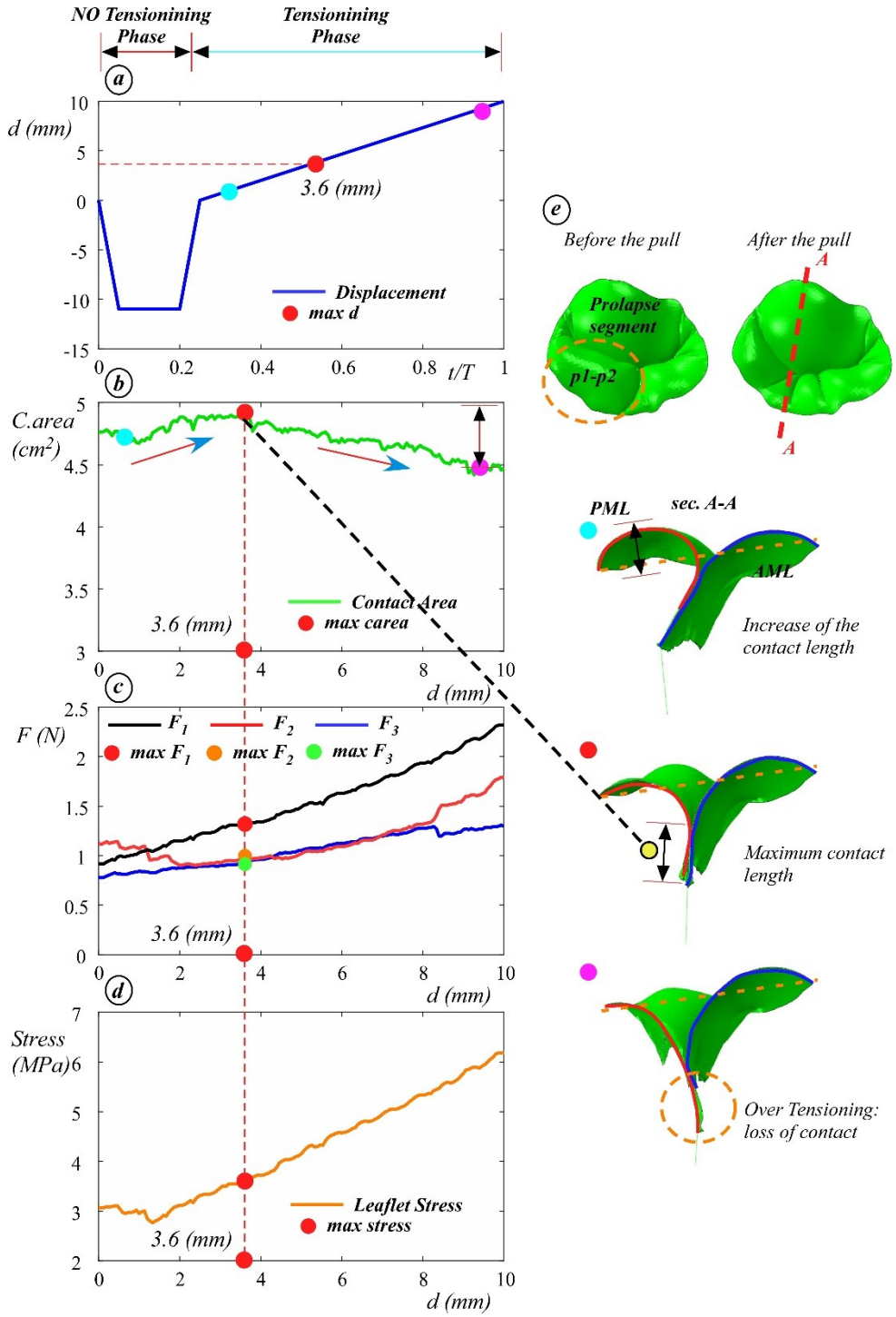

Figure 4-6 *Numerical result for the case A1 with Barlow's disease: panel a) displacement imposed in the simulation; b) the computed contact area in relation with the displacement during the tensioning phase (the red circle indicates the computed maximum area with the displacement of 3.6 mm; c) computed forces for each chordae during the linear displacement (the red, orange and green circles indicate the evaluated forces when of the maximum contact area is attained for the chord 1,2 and 3, respectively; d) evaluation of the additional leaflet stress during the linear displacement; e) Top-view and axis-view of the MV that schematically describe the effect of the pulling.*

The panel a, of Figure 4-6 describes the displacement of the artificial chords as a function of the simulation time. From 0 to 0.2 *t/T* the chords show negative movements due to the preliminary phase of the implants in which the suture are not tensioned. During this phase,

the diseased portion of the posterior leaflet is free to move toward the atrium causing the simulated prolapse condition. At the same time, the pressure condition raises from zero to the maximum pressure of 120 mmHg. Once the maximum pressure and the maximum prolapse are achieved, the sutures are pulled linearly towards the maximum value of 10 mm. In this period the pressure is maintained constant at the systolic maximum pressure.

The panel b shows the evaluated contact area (cm^2). The maximum of this parameter, highlighted by the circle, characterizes the supposed best closure of the valve. In fact, the contact between the anterior and posterior leaflet is indicative of the effectiveness of the repair since it is related to the amount of overlaps between the leaflets during the chords-pulling. As it is possible to observe the computed contact area increases until its maximum is reached (red circle at 3.6 mm). By still increasing the chords displacement, the computed contact area slightly decreases due to the loose of contact between leaflets for the excessively pulling of the sutures. The reduction of the contact area, albeit very small, results into a larger mechanical stress on the leaflets, as clearly pointed out in Figure 4-6 d, that shows a quasi-linear relationship between the maximum stress computed and the chords movement.

The panel e of Figure 4-6 displays qualitatively the simulated leaflet coaptation during the main phases of the pull. The axis view shows the relative position of the posterior leaflet (red line) in comparison to the anterior (blue line). During the first part of the simulation, the posterior leaflet moves freely towards the atrial side, resulting in a consistent amount of prolapse area (light blue circle). The chords tensioning moves the posterior leaflet more toward the ventricular side increasing the leaflets overlap, i.e. increasing also the coaptation length. The maximum contact area is reached when the posterior leaflet free margin reaches the anterior leaflet free margin (red circle). The excessive pull, as indicated in the figure, generates a loss of contact in the opposite direction, with the generation of the so-called virtual prolapse of the anterior leaflet (violet circle) associated to a consequent loss of coaptation length.

The maximum contact area permits to identify the maximum displacement required for the reduction of the prolapse and consequently the proper force and the additional leaflet stress. The force reported in Figure 4-6 c is the forces that each suture exerts on the leaflet in order to restore the valve function. Later, we use all these quantities to compare all the scenarios evaluated. In particular, we refer to the best restoration condition highlighted by the circles red in Figure 4-6.

4.6.2 Patient-specific results: Working angle and device effect

The present section is focused on the role played by the access site position for treating the three typologies of prolapse presented. In accordance with the previous results, each chart shows, for all types of prolapse, the results in terms of Contact Area, the total force due to the tensioning, and maximum additional leaflet stress for both access site angles and leaflets' sutures position.

In this case, all the parameters are plotted (see Figure 4-7) as a function of the working angle (left and right side) for both the neochord and harpoon techniques. i.e. by analyzing different attaching points, in order to analyzed all the possible combinations of MV anatomy and technical repair.

The idea is to understand if geometrical characteristics can influence the results of the restore and/if it is feasible to optimize the procedure, acting on the device or implant characteristics.

The benefit of the implantation of the chords following the neochord and the harpoon procedures in presence of the FED, the Forme Fruste, and the Barlow prolapse are reported in Figure 4-7. As it is possible to observe from the results presented for both the approaches of repairing, the contact area is rather constant, regardless of the working angle adopted in the simulation (panels a), this statement is consistent for all the prolapse types. It is worth noting that differences in terms of absolute value of contact area can be recognized if we compare the computed results between the two different leaflets attaching position, resulting than the NeoChord system expresses larger values than Harpoon device, (about 15 % for all the analyzed cases). The difference in terms of contract values between prolapse depends on the different sizes of the structure of the valves (see Table 4-1).

The achieving of the maximum contact area for all the schemes analyzed determines interesting results in terms of forces (panels b), and leaflet additional stresses (panels c).

In particular for both the devices, in order to completely restore the valves, the force required seems to increase if the sutures trajectories work with large values of α, i.e. when the anterior access location *(α=40°)* is adopted. Such increment of the tensioning is evident in case of neochord implantation, whilst insignificant variation is noticed in the harpoon approach.

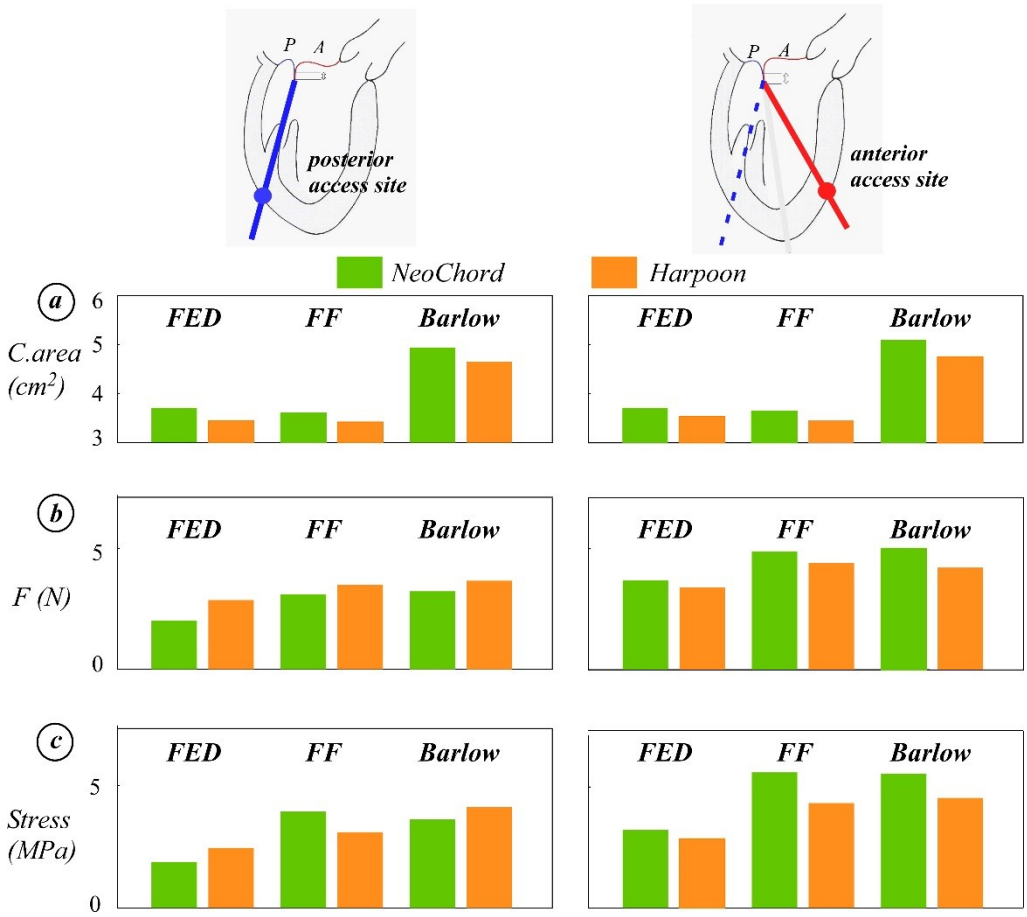

Figure 4-7 *Results in terms of Contact area (panel a), Tensioning Forces (panel b) ad Maximum Additional Stresses (panel c) for both NeoChord and Harpoon leaflet grasp and for different entry site (**left: posterior access, right: anterior access**) for all types of prolapse (FED, FF and Barlow).*

Interestingly, regardless of the type of disease, when the access of the implant is posterior, the use of the harpoon results into a more accentuated force with respect to the neochord. Conversely, with an anterior access, the opposite condition is observed.

The tensioning force is correlated with the additional stress on the leaflet. Also, in this case, the increment of the working angle generates increments of additional stress for both devices and types of prolapse (see panel c).

The harpoon approach, for a posterior access, shows a greater additional maximum stress in accordance with a greater force required. This statement seems not valid for the Forme Fruste prolapse, in fact, for the FF model the analysis of the maximum stress reveals that for both the devices, the anterior access site produce a greater stress, and this additional stress is, for both trajectories, superior by adopting the Neochord approach with respect to Harpoon.

For both FED and Barlow models the maximum stress increases from posterior to anterior access and the neoachord approach indicates a lower stress with posterior access, but different behavior with an anterior access compared to harpoon.

These analyses confirm that important and significant differences are determined by the working angle and by the corresponding trajectory of the artificial sutures implanted. In presence of the Barlow prolapse, we extend the analysis on the effects of the working angle for the neochord procedure, by considering additional access sites located at 20° and 50° with respect to the posterior access (see Figure 4-8).

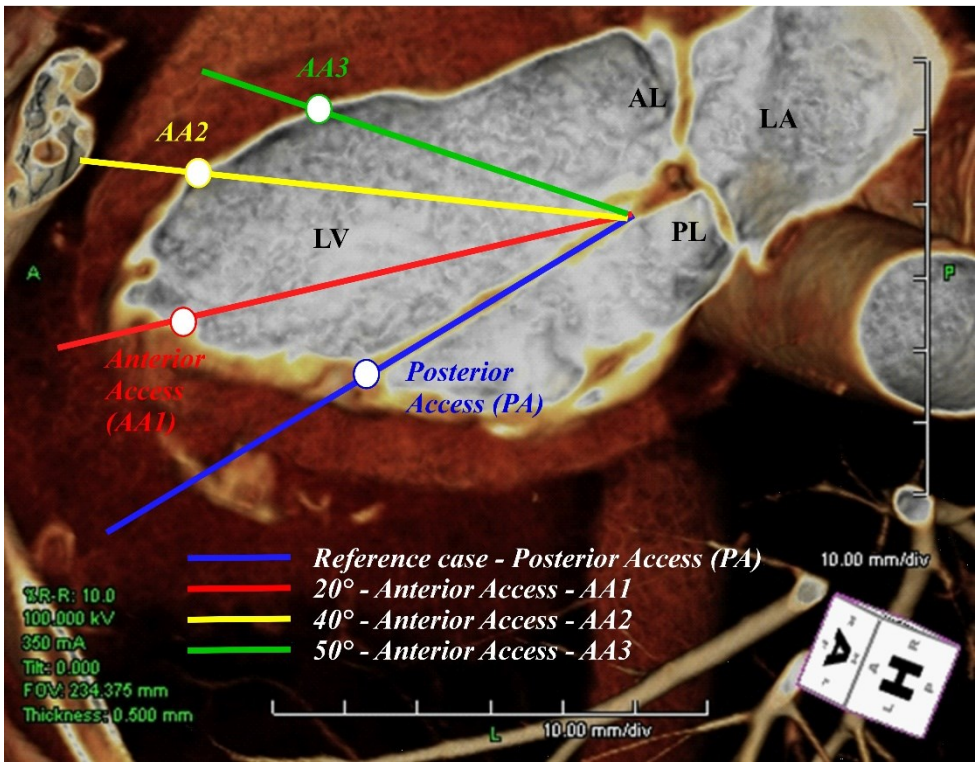

Figure 4-8 *Schematic description of the working angles analyzed. The trajectorieswas moved more anteriorly from the reference working angle (0° - posterior access). Was investigated all the possible scenarios in terms of angles for the repair of the posterior prolapse. This kind of analysis was performed for Barlow's disease and for the NeoChord stitching point.*

The results, reported in Figure 4-9, indicate that, when the working angle ranges between 0° and 40°, the computed contact area is rather constant (about 5.0 cm^2). Interestingly, a further increase of the angle reveals a reduction of this value of about 10 %. This could be explained by an un-physiological shape assumed by the posterior leaflet that, moving more anteriorly, is prevented in the movement by the anterior leaflet.

The displacement and the force required for the complete closure of the valve increase slightly from 0° to 20°, while they increase of about 50% with an access position more anterior, i.e. α=40°. Both these quantities decrease when we further increase the angle to 50°; In terms of displacement, such reduction is very slight, whereas the total force decreases more consistently (about 15%). This condition could be due to the increase of the force due to the contact with the anterior leaflet as shown in Figure 4-10.

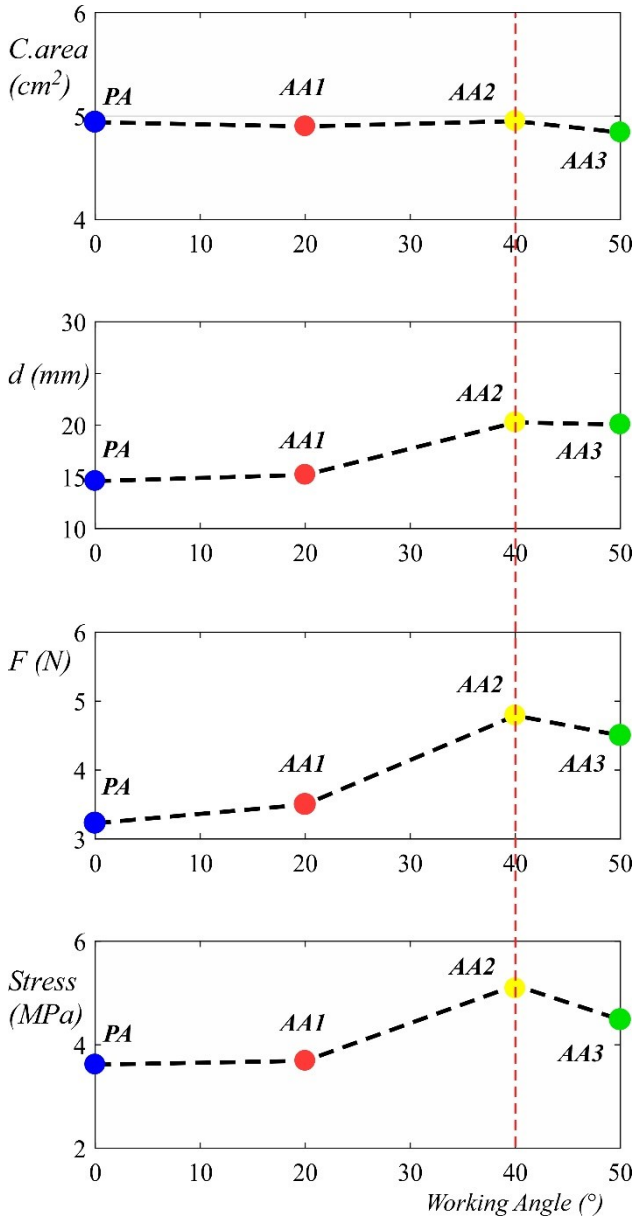

Figure 4-9 *Results of the working angles analysis for the Barlow's disease and for the NeoChord stitching point. From the top to the bottom the results are expressed in terms of Contact Area, Maximum Displacement, Tensioning Forces and Additional Maximum Leaflet Stresses. All these quantities are expressed following the angle variation from 0° to 50°.*

The maximum stress at the attached points varies with the increasing of the working angle similarly to the variation observed for the total force. In addition, in this case, the maximum working angle analyzed $\alpha=50°$ shows a decrease in the maximum leaflet stress.

With high working angle, superior to $\alpha=40°$, the coupling of the artificial sutures with the other structure of the MV may play a significant role to change the final configuration. Apparently, with a working angle superior to 40°, the total forces and the maximum additional stress decrease, and this occurrence could be interpreted positively. However, the evidence of a contact area reduction, as well as the possibility of a disadvantageous

interference with the other substructure of the MV apparatus, suggest to pay attention in restoring the valve through an excessive anterior access site.

A quantification of this unwanted interference among the artificial sutures and the anterior leaflet is performed by a further series of simulations aimed at determining the contact pressure among sutures and anterior leaflet. The results indicates, as expected, that the increase of working angle generate an additional pressure, up to 0.15 MPa, due the contact of the sutures to the anterior leaflet (see Figure 4-10). Here, although the vale is shown in the open position, the color map highlights the value computed at the systolic peak when it is reached the maximum contact area, as described previously. From panel, a (reference case – $\alpha=0°$) to panel d (anterior access at $\alpha=50°$) is possible noticing the increase of the contact area near to the anterior free margin. Until the access site is set in the posterior position the contact among chords and anterior leaflets has the same order of magnitude of the natural contact pressure among all the MV structures. The anterior access site generates an un-physiological impact that may, due to the cyclical nature of the MV dynamics, generate the tearing of the anterior leaflet, [13].

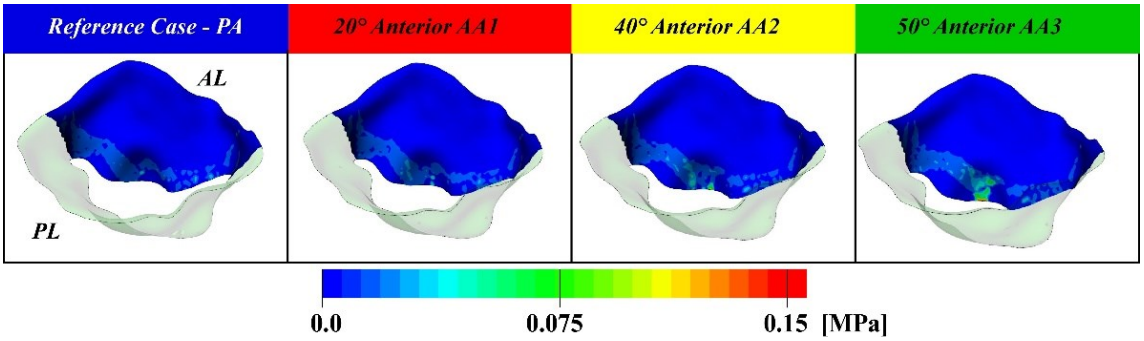

Figure 4-10 *Analysis of the pressure contact between artificial sutures and anterior leaflet; For all the trajectories evaluated the contact between the two elements was evaluated. The colour map highlights the value computed at the systolic peak when the maximum contact area is reached. The results for all the trajectories form α=0° to α=50° area indicated from left to right.*

4.7 Conclusion

The present study analyses the entire scenarios of the posterior prolapse. A different stress and force distribution and final consideration may be expected for the anterior (A) prolapse. In particular, in the latter, due to its different geometry and structural position, the access site and stitching position could be likely to influence the final results here presented.

The present investigation compares the two most common sutures trajectories adopted in the transapical neochords implantation for mitral valve prolapse repair, with the two devices mostly used in the clinical practice. The study was performed with MV patient-specific

morphology, with posterior prolapse. Although simplified constitutive model was assumed, the comparative study describes some preliminary clinical effects of the use of the NeoChord and Harpoon devices.

The repaired configuration obtained for all investigated approach and entry site confirms the reliability and efficacy of the surgical choices in terms of a number of artificial sutures and entry site selection to treat the prolapses here considered. In particular, all the scenario previously describe confirm a re-creation of a physiological condition with all the technical modification adopted, This result is confirmed by the restoration of the optimal contact length for all the models. The differences found in terms of maximum stress distribution and force on the sutures suggest that the two methods of the implant have to be carefully chosen as a function of the entry site, as well as the prolapse type. All the analysis confirm that the NeoChord approach is the most suitable solutions to reach maximum coaptation and maintaining operative leaflets stresses if used with a posterior entry site. On the contrary, albeit with greater absolute values in terms of the quantities analyzed, the Harpoon system experience better results if used with an anterior access entry site.

The presented methodological approach, although with some limitation in terms of boundary condition and material description, was used to highlight potential critical issues derived from different choices due to different technical aspects. Adopted with patient-specific cases, paves the basis for a first computation methodology that can be used as clinical planning tools for a possible implant and restoration design.

4.8 Reference

[1] F. V. Adams DH, Rosenhek R, "Degenerative mitral valve regurgitation: best practice revolution," *Eur Hear. J.*, vol. 31(16), pp. 1958–66, 2010.

[2] P. Lancellotti, M. Radermecker, R. Durieux, T. Modine, and C. Oury, "Transapical beating-heart chordae implantation in mitral regurgitation : a new horizon for repairing mitral valve prolapse," vol. 8, no. 8, 2016.

[3] A. Colli *et al.*, "Transapical off-pump mitral valve repair with Neochord Implantation (TOP-MINI): step-by-step guide," *Ann. Cardiothorac. Surg.*, vol. 4, no. 3, p. 295, 2015.

[4] G. Gerosa, A. D. Onofrio, L. Besola, and A. Colli, "Transoesophageal echo-guided mitral valve repair using the Harpoon system," vol. 53, no. October 2017, pp. 871–873, 2018.

[5] A. Colli *et al.*, "CT for the Transapical Off-Pump Mitral Valve Repair With Neochord Implantation Procedure," *JACC Cardiovasc. Imaging*, vol. 10, no. 11, pp. 1397–1400, 2017.

[6] A. Atehortua, M. A. Zuluaga, J. D. Garcia, and E. Romero, "Automatic segmentation of right ventricle in cardiac cine MR images using a saliency analysis," *Med. Phys.*, vol. 43, no. 12, pp. 6270–6281, 2016.

[7] K. May-Newman and F. C. Yin, "Biaxial mechanical behavior of excised porcine mitral valve leaflets," *Am. J. Physiol. Circ. Physiol.*, vol. 269, no. 4, pp. H1319--H1327, 1995.

[8] K. Kunzelman, M. S. Reimink, E. D. Verrier, R. P. Cochran, and R. W. M. Frater, "Replacement of Mitral Valve Posterior Chordae Tendineae with Expanded Polytetrafluoroethylene Suture: A Finite Element Study," *J. Card. Surg.*, vol. 11, no. 2, pp. 136–145, 1996.

[9] K. D. Lau, V. Diaz, P. Scambler, and G. Burriesci, "Mitral valve dynamics in structural and fluid-structure interaction models," *Med. Eng. Phys.*, vol. 32, no. 9, pp. 1057–1064, 2010.

[10] H. Muresian, "The clinical anatomy of the mitral valve," *Clinical Anatomy*, vol. 22, no. 1. pp. 85–98, 2009.

[11] E. Votta, E. Caiani, F. Veronesi, M. Soncini, F. M. Montevecchi, and A. Redaelli, "Mitral valve finite-element modelling from ultrasound data: a pilot study for a new approach to understand mitral function and clinical scenarios," *Philos. Trans. R. Soc. A Math. Phys. Eng. Sci.*, vol. 366, no. 1879, pp. 3411–3434, 2008.

[12] I. S. Salgo *et al.*, "Effect of annular shape on leaflet curvature in reducing mitral leaflet stress," *Circulation*, vol. 106, no. 6, pp. 711–717, 2002.

[13] A. Colli *et al.*, "Transapical off-pump mitral valve repair with Neochord implantation: Early clinical results," *Int. J. Cardiol.*, vol. 204, pp. 23–28, 2016.

5 CONCLUSION AND FUTURE WORKS

5.1 Conclusion

The present work focuses on the numerical analysis of a new mini-invasive technique, the Transapical NeoChord Procedure. This new approach, able to mitigate the mitral valve regurgitation, consists of the implantation of artificial sutures (e-PTFE) with a beating-heart approach by a suitably designed delivery system (NeoChord Device DS1000), with the aim of restoring the physiological closure of the mitral valve.

It was developed a first numerical analysis able to describe and evaluate some of the critical aspects that surgeons have underlined during the performing of the repair, such as, the tensioning protocols and the entry site analysis.

In Chapter 4 we presented a first numerical investigation concerning the comparison of two of the most common tensioning procedures adopted in the transapical neochords implantation, the so-called 'all together- AT' and 'one by one – 1by1' pulling approach. For the comparative nature of the study, a generalized MV morphology affected by a central posterior leaflet (P2 scallop), i.e., the most common leaflet disease, was adopted.

Both strategies were compared in terms of *i)* coaptation area, defined as the index of closure due to the amount of overlaps between leaflets, *ii)* additional leaflets stress due to the suture leaflets stitching, and *iii)* tensioning forces. In addition, in order to evaluate the efficacy of the restoration due to the chords implant, all the virtual tensioning simulations were compared with a healthy MV configuration, in which there is not the presence of the prolapse.

Our analyses suggest that the 1by 1 repair is the most suitable solutions to reach maximum coaptation and to maintain operative leaflets stress close to those experienced in healthy condition and, although idealized geometries and simplified constitutive behaviors were assumed, the study captures some of the clinical effects observed by surgeons, e.g. the unloading of previously pulled neochords.

Our study is limited to the prolapse of the posterior leaflet, located in the central segment. Which represents the most common prolapse type. However, the symmetrical configuration of the diseased anatomy analyzed, results more indicative for catching the intrinsic flaws directly related to the tensioning protocol, that is the aim of this preliminary investigation.

Nevertheless, the role of the MV anatomy, as well as of the prolapse location is reported as appendix (see p1-p2 scallops - appendix of Section 3), pointing out the possible

interference of the artificial suture with the native chordae, regardless the tensioning approach adopted.

The use of patient-specific approach is instead presented in the second issue addressed, concerning the analysis of different entry site positions around the apex zone that is necessary for the introduction of the device and different stitching point around the leaflet (Section 4).

All the possible scenarios of the MV prolapse disease and the related numerical analysis are carried out aiming at investigating the performance of the NeoChord and Harpoon devices, currently employed for the repair of the mitral prolapse with the insertion of artificial chordae. Both the devices perform the procedure with different entry sites and stitching point. In particular, the NeoChord implant occurs usually posteriorly stitching the chords on the leaflet free margin, while the Harpoon implant occurs usually anteriorly stitching the chords on the belly body.

The presented patient-specific analysis was able to describe the all spectrum of the MV disease (FED, Forme Fruste and Barlow'disease) in order to evaluate the effect of the geometry on the two procedures.

For each prolapse type, the trajectories of the sutures, starting from a posterior access $\alpha=0°$ to an anterior access $\alpha=40°$, and the stitching point, i.e. sutures grasped on the leaflet free margin or on the leaflet belly, were investigated.

The results suggest that, for the entire prolapse types investigated, the anterior access ($\alpha=40°$) does not increase the contact area and, consequently, does not improve the valve closing, while it determines an increment of both the tensioning forces and the additional stress around the stitching leaflet points. The belly insertion, mainly related to the Harpoon approach, shows a decreasing of the contact area for both the entry sites, while, with a posterior access, it shows higher values of forces and additional stress in comparison with the NeoChord technique. The opposite results was noticed with an anterior access. This occurrence confirms the validity of the standard technical characteristics suggested by the producers of the devices.

In addition, for a single type of prolapse, i.e. the Barlow's disease, we evaluated the effect of a different fan of trajectories, from $\alpha=0°$ up to $\alpha=50°$, in order to identify the optimum access site position, which minimizes the leaflet stress and maximizes the contact area.

The analysis of the working angle shows no significant difference in terms of contact area, forces and stress for α between 0° to 20°, while increasing the working angle up to 40° we noticed differences of about 50% for all the variables investigated with compared

to the posterior access. Further increasing the working angle up to α=50° a non-negligible reduction was computed in terms of tensioning forces and stress, in addition to a decreasing of the contact area.

By these simulations, we evaluate and quantify one of the critical aspects identified by the surgeons, as, the occurrence of the contact between the artificial sutures and the anterior leaflet when the chords are implanted anteriorly. This event, much more critical for large working angle, leads to unwanted pressure contact that for the cyclical nature of the leaflets dynamic may tear the leaflet itself.

The use of patient-specific anatomy has further improved the results and highlighted other different aspects of the NeoChord implant. In particular, this unwanted interference seems to be more important with MV geometrical characteristics that present a large area of the anterior leaflet. We can speculate that in these conditions the knowledge of the MV structures can address the best technical choice.

The application of these numerical simulations provides a useful tool for procedural planning, improving, in such a way, the efficacy of the treatment.

In addition, this kind of tool could be used not only for confirming, the already known methodological approaches and the differences among technical chooses, but also for evaluating and providing new technical solutions in terms, for example, of device design.

We believe that the robustness and the reduced computational cost of the presented methodological approach make the model suitable to be adopted for the clinical planning.
Future Work

All the numerical simulations presented simplified mechanical characteristics, boundary conditions, and pressure load. A better quantification of the impact on the results due to these simplifications could help to further improve our methodology.

In terms of boundary conditions, the methodology discussed in Section 4, which is based on the analysis of the clinical data for the design of the MV anatomy, permits to define quite accurately all the dynamic components of the mitral valve sub-structures and, in the short term, it could be implemented for improving our knowledge on the tensioning manoeuvre and final neochord's trajectories.

The results in terms of forces here presented have been partly confirmed from some experimental experiences performed by Bajona and co-workers that have evaluated the force requires for the restore of an anterior prolapse by means of an experimental simulation of the implant with a porcine MV.

The reliable validation of our result could be performed thanks to the implementation of a workbench in vitro model able to reproduce the boundaries conditions simulated in the numerical analysis.

With the aim to better design the clinical approach depending on the different MV characteristics, our imminent future work will be to extend the numerical model here presented toward a population-specific approach. The advantages are the generalization of the implant features for large classes of patients affected by MV prolapse and thus the possibility of providing guidelines for their treatment.

Thanks to the developing of a new tool (shape analysis), proposed by our collaborators at UCL (B. Biffi and S. Schievano), for the creation of 3D MV geometries, will be possible converting complex clinical data in a 3D representation of the MV. Statistical shape analysis represents an innovative quantitative tool based on 3D anatomical data that can guide in patients stratification and procedure planning. Moreover, the average MV shape and the information on shape variability can be used by designers to optimize any device based on population-derived anatomies.